DROUGHT, TREE MORTALITY, AND REGENERATION IN NORTHERN CALIFORNIA

By

Sophia Lemmo

A Thesis Presented to

The Faculty of California State Polytechnic University, Humboldt

In Partial Fulfillment of the Requirements for the Degree

Master of Science in Natural Resources: Forestry, Watershed, and Wildland Sciences

Committee Membership

Dr. Lucy Kerhoulas, Committee Co-Chair

Dr. Rosemary Sherriff, Committee Co-Chair

Dr. Erik Jules, Committee Member

Dr. Christopher Lee, Committee Member

Dr. Erin Kelly, Graduate Coordinator

May 2022

ABSTRACT

DROUGHT, TREE MORTALITY, AND REGENERATION IN NORTHERN CALIFORNIA

Sophia Lemmo

The 2012-2016 California drought was the most severe in the state's recorded history, contributing to the death of millions of trees. While the effects of this drought on forests are relatively well studied in the central and southern Sierra Nevada, less is known about its effects on the heavily timbered and diverse forests of northern California. Through sampling 54 0.25 ha plots in northern California, this study compared tree mortality and regeneration patterns before, during, and after California's most recent record-setting drought. This study evaluated 1) the influence of habitat and competitive covariates on mortality and regeneration trends using ridge regression analysis; and 2) tree death and seedling/sapling establishment dates using dendrochronology and Superposed Epoch Analysis to explore the influence of climate on forest demographics. Montane drought-induced tree mortality occurred primarily in trees smaller than 40 cm diameter at breast height (DBH), with no coastal drought-related mortality in trees with DBH greater than 80 cm. The highest rates of overstory mortality across all sites were observed in *Abies grandis* (51%), *Pinus lambertiana* (43%), and *Pinus monticola* (37%). *Picea breweriana* (6%) and *Picea sitchensis* (9%) had the lowest average mortality rates.

In montane environments, years with high rates of mortality were positively associated with climatic water deficit (CWD; drier than expected conditions) in the 1-2 years preceding and during tree death dates. Pre-drought montane mortality was greater at wet sites than dry sites, and recent montane mortality (~2013-2020) was positively related with canopy openness. In coastal environments, recent tree mortality was positively associated with maximum temperature and topographic position. Regeneration was dominated by advanced regeneration (median age of 32 years) of shade-tolerant species. In montane environments, regeneration dates were significantly associated with lower-than-average CWD the year proceeding. In coastal environments, regeneration was greater at dry sites than wet sites, and was positively associated with stand density and maximum temperature. These data demonstrate that these forests are not actively perpetuating as diversely into the future, especially in montane environments where more mortality is found in white pine species (*Pinus lambertiana* and *P. monticola*) and where the regeneration is weighted towards advanced regeneration of shade-tolerant fir species. This work indicates a need to implement targeted management aimed at generating disturbances to foster balanced and responsive regeneration. This management should preferentially retain medium to larger trees, as these size classes seem to be the least vulnerable to mortality. Such management would be promising for supporting the resilience and diversity of northern California landscapes.

ACKNOWLEDGEMENTS

This study was supported through several funding sources including the USDA National Institute of Food and Agriculture McIntire-Stennis Project (CALZ-168), the National Science Foundation (NSF) – Geography and Spatial Sciences (GSS) Program (BCS-1853903), the California State Agricultural Research Institute, the North Coast Chapter of California Native Plant Society, Northern California Botanists, Cal Poly Humboldt Student Opportunity Fund, and the Robert Powers Memorial Scholarship Program. To my advisors, Dr. Lucy Kerhoulas and Dr. Rosemary Sherriff, thank you for your tireless support, mentorship, and encouragement, especially in widely disseminating my findings. I also acknowledge and thank my other thesis committee members for their support throughout this process: Dr. Erik Jules and Dr. Christopher Lee. An extra thanks to Dr. Lee who came all the way out to Etna, CA to lend a hand with fieldwork and show us some local insects and pathogens. Additionally, this project would not have been possible without field and lab assistance from several Cal Poly Humboldt undergraduates including Rosalio Gonzalez, Jennah Brown, Charles Russell, and Britney Martinez. Thanks to Kelly Watson of Cal Poly Humboldt for providing crucial Windendro and COFECHA support and skill. Thanks to Jill Beckmann of Northern Arizona University who worked endlessly to help me with statistics and R; I do not know where this project would be without her expertise. Thanks to Dr. Andre Buchheister and Dr. Mark Henderson for being expert sounding boards on statistical approaches. Thanks to the various landowners and their representatives for granting access to study sites including

the National Park Service, California State Parks, the U.S. Forest Service, Humboldt Wildlife Refuge, and the City of Arcata. Thanks to Wallis Robinson and Gabriel Roletti for sharing a lab space and for providing advice. Finally, thanks to Sarah Aguiar, Perris Alfonzo, Sara Bandali, Jeremy Dustin, Maeve Flynn, Gabriel Goff, Suzanne Melendez, and Ashley Shannon for helping early on with field work.

TABLE OF CONTENTS

LIST OF TABLES

LIST OF FIGURES

LIST OF APPENDICES

INTRODUCTION

The 2012-2016 drought in California ranks as the most severe in the state's recorded history (Griffin and Anchukaitis, 2014; Williams et al., 2015), with the current drought (2021-present[2022]) ranking second so far. The frequency of droughts in California has increased over the last century (Hughes and Brown, 1992), and the rate and duration of droughts are expected to increase as a result of climate change (Diffenbaugh et al., 2015; Meehl and Tebaldi, 2004). Drought reduces tree hydraulic function, carbon fixation, and capacity to translocate photosynthate (Hartmann, 2015; McDowell et al., 2008; Sevanto, 2014), consequently decreasing radial growth and increasing susceptibility to forest insects and diseases (Allen et al., 2010; Stephenson et al., 2019). This process of interacting agents leading to tree mortality has been dubbed the "decline disease spiral" (Manion, 1981), where predisposing factors such as site characteristics (e.g., dry-wet moisture regimes, stand density), and inciting (e.g., drought) and contributing (e.g., pathogens and pests) factors all play a role in the death of a tree. Warmer winter temperatures associated with drought allow forest pests to thrive (Breshears et al., 2005; Logan et al., 2003). Thus, the recent 2012-2016 California drought was an inciting factor that led to the contributing factors of forest insect and pathogen outbreaks, resulting in extensive mortality. In extreme events, drought alone can lead to mortality through hydraulic failure and/or carbon starvation (McDowell, 2011). Tree death turns total live "green" fuels into available fuels, which can increase the risk for wildfires (Stephens et al., 2018). Intense drought can also lead to increased

canopy water stress (Asner et al., 2016), a predictor of vegetation flammability (Ustin et al., 2004), and to drying in the deep-rooting-zone, further contributing to tree die-off (Goulden and Bales, 2019). The compounding effects of drought, forest pests, and wildfire have led to the death of over 150 million trees across the state as of 2019 (USDA, 2020).

The effects of the 2012-2016 drought have been comprehensively studied in the more populated and arid regions of the southern and central Sierra Nevada (Asner et al., 2016; Byer and Jin, 2017; Das et al., 2016; Dong et al., 2019; Stephens et al., 2018; Stephenson et al., 2019; van Mantgem et al., 2016; Young et al., 2020, 2017). In some regions and among some species, more than 50% of trees died (Fettig et al., 2019; Stephenson et al., 2019). Comparatively few studies of forest responses to drought have included regions of northern California (except see Asner et al., 2016; Bost et al., 2019; DeSiervo et al., 2018; Dong et al., 2019; Vernon et al., 2018; Young et al., 2017). One such study found that across California, the highest rates of tree death occurred in 2015 and 2016 (the fourth and fifth consecutive year of drought, respectively) (Byer and Jin, 2017), indicating a possible lagged mortality response to drought (Das et al., 2013). While vegetation in northern California was less affected by the drought and experienced less forest mortality than other regions in the state (Dong et al., 2019), northern California forests still experienced detrimental drought impacts. For example, in the Russian Wilderness of the Klamath Mountains, a recent study found 22% of the trees died (DeSiervo et al., 2018). However, unlike the 2012-2016 drought, the current drought (2021-present [2022]) is more extreme in portions of northern California than in the

Sierra Nevada (U.S. Drought Monitor, 2022). As such, in 2021, the Shasta-Trinity National Forest had the highest number of acres with tree mortality across all National Forests in the state (USDA, 2021).

Tree decline and mortality from drought differ among species, size classes, stand densities, and habitats. Increased forest density is a consistent predictor of higher mortality levels across California (Das et al., 2011; Fettig et al., 2019; van Mantgem et al., 2016; Young et al., 2017). Climatic water deficit (CWD) can also be a predictor of mortality, particularly as droughts progress, and with the presence of high live basal areas (Young et al., 2017). In fact, high density (>30 m^2 ha^{-1}) stands with only moderately high CWD still experienced substantial mortality during the recent drought (Young et al., 2017). Therefore, management techniques such as thinning and prescribed fire that reduce forest density have the potential to improve forest drought resistance and resilience (Stephens et al., 2020; van Mantgem et al., 2016; Vernon et al., 2018). However, these treatments have varying effects on species' ability to resist insect attack, with prescribed fire increasing beetle infestation in red fir (*Abies magnifica* A.Murray) and sugar pine (*Pinus lambertiana* Douglas) in some instances (Steel et al., 2021). Among habitats and species in the Sierra Nevada, mortality was highest at low to mid elevations (Byer and Jin, 2017; Fettig et al., 2019), and was most prominent in *Pinus* species (Fettig et al., 2019; Stephenson et al., 2019) and white fir (*Abies concolor* (Gordon & Glend.) Lindl. ex Hildebr.) (Byer and Jin, 2017). This variability in mortality is likely due in large part to species-specific susceptibility to common insects and diseases (Byer and Jin, 2017; Das et al., 2016; Fettig et al., 2019). Northern California

species that recently experienced die-off events due to heightened susceptibility to insects and pathogens include Shasta red fir (*Abies magnifica* var. *shastensis* Lemmon) and Port Orford-cedar (*Chamaecyparis lawsoniana* A. Murray). In the Russian Wilderness, Shasta red fir mortality was associated with Wien's dwarf mistletoe (*Arceuthobium abietinum* subsp. *Wiensii* Mathiasen & Daugherty), a parasite that was positively associated with fir engraver beetle (*Scolytus ventralis*) infections (DeSiervo et al., 2018). Port Orford-cedar die-off events were attributed to the non-native root rot pathogen *Phytophthora lateralis* (Jules et al., 2014). Mortality rates also vary across tree sizes within a species (DeSiervo et al., 2018; Jules et al., 2014; Stephenson et al., 2019), with higher rates of drought-related mortality generally occurring in medium to large co-dominant and dominant trees (Das et al., 2016; Stephens et al., 2018; Young et al., 2020).

It remains unclear whether drought-associated mortality is amplified by habitat (i.e., dry versus wet habitats). One hypothesis is that trees in wetter sites are adapted to high water availability due to high leaf-area and poor water use efficiency (Clark et al., 2016, 2014; Field et al., 1983), and thus are more vulnerable to water reduction. Supporting this hypothesis, in some cases, trees living in relatively xeric regions of their range fare better during drought than individuals in relatively wetter regions (Orwig and Abrams, 1997). On the other hand, trees in xeric sites may already exist at their limit of water availability (Stephenson, 1990), and in some cases have experienced greater mortality than trees in relatively mesic sites (Young et al., 2017). Given this ambiguity, there is a need to better understand intraspecific drought-induced tree mortality trends across a range of moisture regimes (i.e., dry, moderate, and wet habitats).

After overstory mortality events, including those related to the 2012-2016 drought, forest recruitment, especially advanced seedlings (regeneration established prior to overstory mortality), facilitates recovery (Collins et al., 2021; Kayes and Tinker, 2012; Redmond and Barger, 2013). However, droughts can change where certain species are able to regenerate, leading to shifts in species' abundances and distributions (Allen et al., 2010; Beckage et al., 2008; Stephenson, 1998). To forecast future forest composition trends in northern California, both patterns in mortality and regeneration at stand scales must be understood. On multiple continents, it is more common for new tree and shrub species to dominate regeneration following drought-related overstory mortality, thereby leading to the eventual replacement of the pre-drought dominant species (Batllori et al., 2020). Following drought in the Sierra Nevada, shade-tolerant species are typically the dominant regeneration, particularly in dense stands (Fettig et al., 2019; Young et al., 2020), reflecting a shift in species distribution from historical conditions. The potential shift in forest species composition after drought-related mortality, and the importance of recruitment for stand perpetuation, suggests that an assessment of species-level regeneration in northern California is critical. This information provides insight on future forest demographics in a region where little is known about post-drought regeneration compared to other areas of California.

Many factors can influence forest regeneration: seed trees; cone/flower production; seed production, viability, and dispersal; seed banks; seed predation; advanced regeneration; mycorrhizae; duff; soil; ground cover; shrub cover; and climate, to name a few. For example, under overly warm and dry conditions, regeneration

establishment and survival can be precarious (Kitzberger et al., 2000; Rodman et al., 2020; Sthultz et al., 2007). And certain tree species such as piñon pine (*Pinus edulis* Engelm.) can be more dependent on advanced regeneration for perpetuation after drought-associated overstory die-off than other species (Redmond and Barger, 2013). In some circumstances, growing season precipitation is a strong predictor of tree regeneration, while climatic water deficit (CWD) is negatively associated with successful regeneration (Rodman et al. 2020). Additionally, in the Sierra Nevada, abiotic conditions can be the primary limiting factor for successful forest regeneration (van Mantgem et al., 2006). Thus, it can be challenging to generalize across regions to predict forest responses following drought-related tree mortality. By dating regeneration, patterns between climate and tree establishment in post-drought forest propagation, as well as the relative importance of advanced regeneration, can be better understood.

The goal of this study was therefore to improve understanding about the perpetuation of forest stands in northern California after extended drought by answering the following two research questions:

1) How do tree mortality and regeneration in northern California vary with species, stand density, and habitat before and after extended drought?

2) How do tree mortality and regeneration events in northern California change with climatic water deficit?

2. MATERIALS AND METHODS

2.1 Study Area

The study area includes the forested region of northern California (**Error! Reference source not found.**), a diverse area, capturing a range of environments that span five biotic regions, three biogeographic regions, and three distinct climate gradients. In this area, the Cascades, California Valley, Great Basin, Sierra Nevada, and Coast Range all intersect. Specifically, the study area includes the Klamath Mountains, the area between that range and the Pacific Ocean (the North Coast), and the southern portion of the Cascades. This region therefore supports a mosaic of forest types including coastal redwood forests, coastal coniferous forests, mixed evergreen forests, mixed conifer forests, red fir forests, and subalpine forests (Griffin and Critchfield, 1972), with a distinct difference in species composition between montane and coastal sites. Underlying these forests in the Klamath Mountains and the North Coast is a complex mix of metamorphic bedrock, with some serpentinite and silica-rich formations (DeCourten, 2009). Due the volcanic activity, the southern Cascades contain extrusive formations (DeCourten, 2009). Rich, alluvial soils dominate the North Coast, while gravelly, moderately- to well-drained loamy soils characterize the Klamath Mountains (USDA, n.d.), and the southern Cascades contain moderately-to well-drained volcanic soils (Skinner and Taylor, 2006). The study area also spans land in relationship with many

indigenous communities' traditional and current homelands including the Pomo, Mattole, Wiyot, Karuk, Hupa, Yurok, Tolowa Dee-ni', Lassik, Wintu, Shasta, Modoc, and Maidu tribes ("Northern California Indian Development Council," 2021).

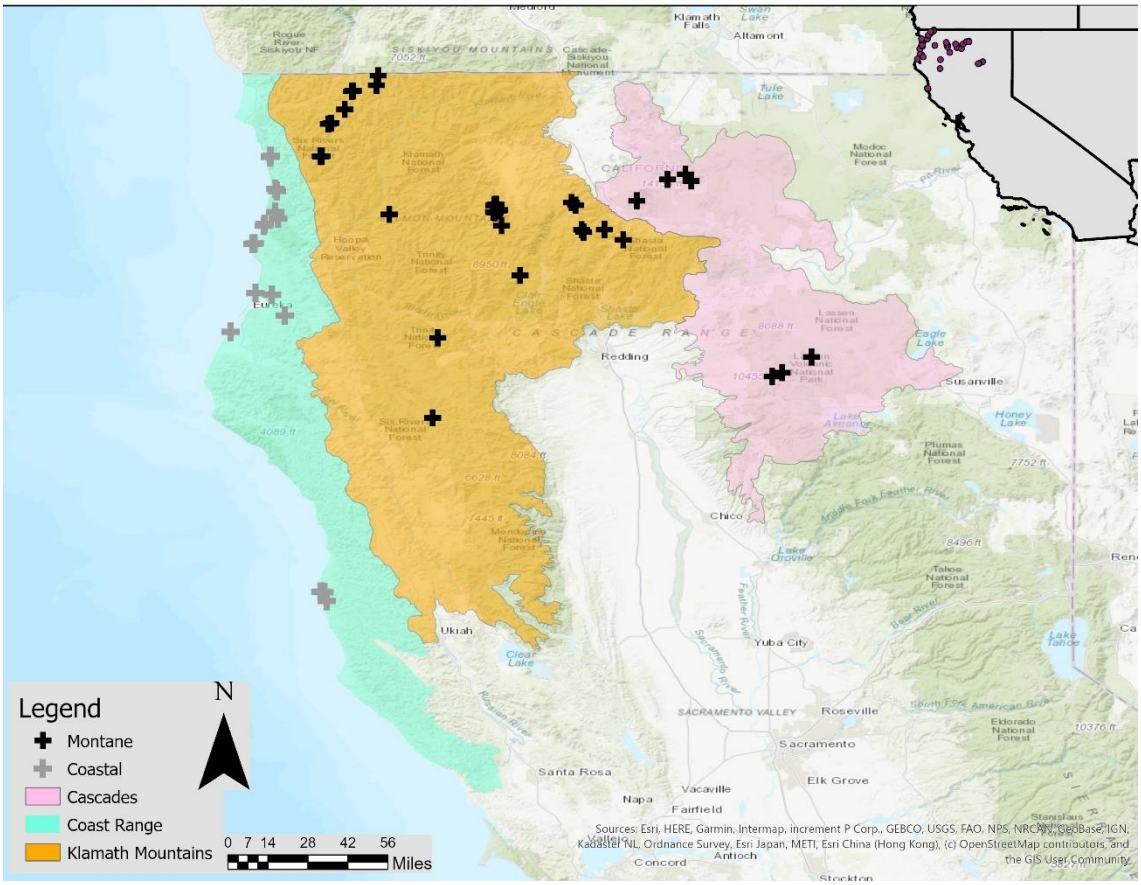

Figure 1. Map of the study area. Plus signs symbolize the locations of 54 study sites across northern California, with grey plus signs indicating coastal sites (n = 18) and black plus signs denoting montane sites (n = 36). Map made with ArcGIS Pro, using level III ecoregion data from the U.S. Environmental Protection Agency (Level III Ecoregions of the Continental United States, 2013).

Overall, the study area can be characterized by a Mediterranean climate with relatively warm, dry summers and cool, wet winters (Robinson, 2021; Sherriff et al., in press; Skinner et al., 2006). The mean annual 30-year precipitation (PPT_{30}, 1990-2020)

for the study sites ranges from 780 to 1,933 mm, the mean annual 30-year minimum temperature ranges from -3 to 8 °C, and the 30-year mean annual maximum temperature ($T_{max,30}$) ranges from approximately 10 to 19 °C, depending on site location (TerraClimate, http://www.climatologylab.org/terraclimate.html). The study sites capture three distinct climate gradients: north-south, east-west, and elevational. From north-to-south there is a gradient of decreasing winter precipitation and warmer summer temperatures, while trending west to east, the climate is affected by proximity to the Pacific Ocean (Sherriff et al., in press; Skinner et al., 2006). The northern coastal rainforests can receive over 2,500 mm of rain, whereas inland lower elevations of the eastern Klamath receive far less precipitation, with the driest region being in the transition zone from the Klamath Mountains into the southeastern Cascades, receiving approximately 533 mm of precipitation annually (Sherriff et al., in press; Western Regional Climate Center, n.d.). Along the coast the temperature is more stable compared to montane regions (TerraClimate, http://www.climatologylab.org/terraclimate.html). Although the coast is more consistently wet throughout the year than the inland mountains, annual precipitation at the coast is relatively lower. However, in recent years (2007-2016), the coastal sites received more annual precipitation than montane sites (Robinson, 2021). Climate also varies from low to high elevations, with the snow level in the study area around 1,500 m (Sherriff et al., in press).

The climatic and geographic diversity of the study area supports high biodiversity. The studies' center region, the Klamath Mountains, is unique for its highly diverse plant taxa; especially notable is the presence of over 30 conifer species (Kauffmann, 2012;

Whittaker, 1961, 1960). The high number of endemic species and species diversity are due in part to the highly variable climate present within the study area.

The current stand densities and species compositions of the study sites reflect the effects of increased fire return intervals. Pre-Euro-American colonization, natural and cultural fire regimes in northern California, and especially in the Klamath Mountains, contributed to the region's plant diversity and heterogeneous forest structure (Knight et al., 2022; Skinner et al., 2006; Taylor and Skinner, 1998). The area was predominantly characterized low to moderate severity fires (Taylor and Skinner, 1998). However, since the 1900s, Euro-Americans participated in fire suppression and other land use activities, altering densities and species compositions, which are now reflected across the study area (Knight et al., 2022; Miller et al., 2017). In turn, this management has increased shade tolerant species, and, in some regions, decreased species diversity.

2.2 Field Sampling

To quantify forest mortality and regeneration in northern California, 54 sampling locations (Figure 1) were selected based on an ongoing complementary study (Robinson, 2021; Roletti, in press) examining the influences of competition and habitat on drought responses (annual growth and ^{13}C in tree-rings) of six northern California conifer species (Appendix A). The complimentary study used observational data from Calflora (http://calflora.org), along with local expert suggestion (Michael Kauffmann, pers. comm) to locate potential sites (see Robinson 2021 and Roletti 2022). Although study

sites were selected based on six focal conifer species (Brewer spruce (*Picea breweriana* S. Watson), Shasta fir, Sitka spruce (*Picea sitchensis* (Bong) Carr), sugar pine, western hemlock (*Tsuga heterophylla* (Raf) Sarg), and western white pine (*Pinus monticola* Douglas ex D. Don)), this current investigation measured forest demographic trends for all tree species encountered within plots. The sites ranged from dry to wet (based on PPT_{30}, PRISM), with three replicate sites per moisture regime (dry, moderate, and wet) for each of the complementary study's focal conifer species (54 sites total), thus capturing a broad range of climatic conditions. Although 54 sampling sites cannot encompass the full range of diversity throughout the region, the sites adequately capture the diversity of forest stands and environmental conditions across the habitat ranges of the six focal conifer species within their northern California range. Sites were chosen to ensure that each location experienced the 2013-2015 drought, confirmed by a low (i.e., $\leq$ -2) 2014 Palmer Drought Severity Index (PDSI) value. Care was also taken to verify that sites had not experienced fire or logging activities in the last 50+ years. Lastly, serpentine soils were avoided when possible.

Field sampling occurred in the summers of 2020 and 2021. Each of the 54 sites were established by a random azimuth offsetting 20 m from the pre-existing site coordinates of the complementary study. At each site, a 0.25 ha plot, with a nested 0.1 ha subplot, was established to measure tree mortality and regeneration, respectively. To avoid conflating the effects of measured covariates with other factors, all plots were greater than 5 m from watercourse channels, wet seeps, lakes, roads, trails, and parking lots.

Slope, aspect, topographic position, stand characteristics, and evidence of disturbances were determined for each plot using professional judgment and a clinometer when appropriate. Ground cover was ocularly estimated and canopy cover was measured using a spherical densiometer at plot center and halfway out the radius of the plot in each cardinal direction. To quantify stand density, each live tree over 5 cm in diameter at breast height (DBH, 1.37 m) was measured within the 0.1 ha subplot. To initially differentiate between tree death due to natural thinning/suppression (Peet and Christensen 1987) versus other factors, trees 4-10 cm DBH were tallied by diameter, species, and status (live/dead). Trees with DBH's greater than 10 cm are hereafter referred to as overstory trees. For all live overstory trees within the 0.1 ha subplot, species, DBH, status (live/dead), damage (e.g., insects, disease, broken top), decay class (if dead), and vegetative cover within 5 m were recorded. Crown classifications for live trees were recorded (Schriver et al., 2018; Wright et al., 2018), but not used. To ensure enough dead trees were captured, all dead trees greater than 10 cm DBH were measured and recorded throughout the entire 0.25 ha plot.

Dead trees were sorted into one of five decay classes based on prior studies (Fogel et al., 1973; Harmon et al., 2011) (Appendix B). Fallen and downed trees were not considered as part of the dead tree count. To establish the death date, two trees per species and decay class per plot, when present, were sampled with a 5 mm increment borer. Due to high decomposition of trees in decay classes four and five, it was not possible to extract intact cores from those trees. Cores from coastal environments tended to be crumblier than those from montane environments and were less successfully

sampled. Live tree cores taken by the complementary study at the same sites were used for crossdating the dead trees using standard methods (Speer, 2010).

Regeneration was assessed by counting all seedlings (< 30 cm tall) and saplings (> 30 cm tall and < 4 cm DBH) in each 0.1 ha subplot and sorting them by height size classes (< 15 cm – seedling I, 16-30 cm – seedling II, 30-137 cm – sapling I, and > 137 cm – sapling II). These size classes were adapted from seedling heights used in the U.S. Forest Service Forest Inventory and Analysis Program field protocols (U.S. Department of Agriculture and Analysis, Forest Service, 2016). Five basal disks per species were cut from seedling/sapling root crowns and collected to date regeneration ages. The five samples included regeneration closest to the plot center and the plot edge in each cardinal direction. Standard dendroecological techniques were used to date the time of establishment (Holmes, 1984).

2.3 Selection of Drought Period

To define the drought period within the study area, mean annual PDSI values were calculated based on monthly values obtained from TerraClimate (http://www.climatologylab.org/terraclimate.html). Across sites, 2012 and 2016 generally had PDSI values above -2 ( ), and thus, the drought period was defined as 2013-2015.

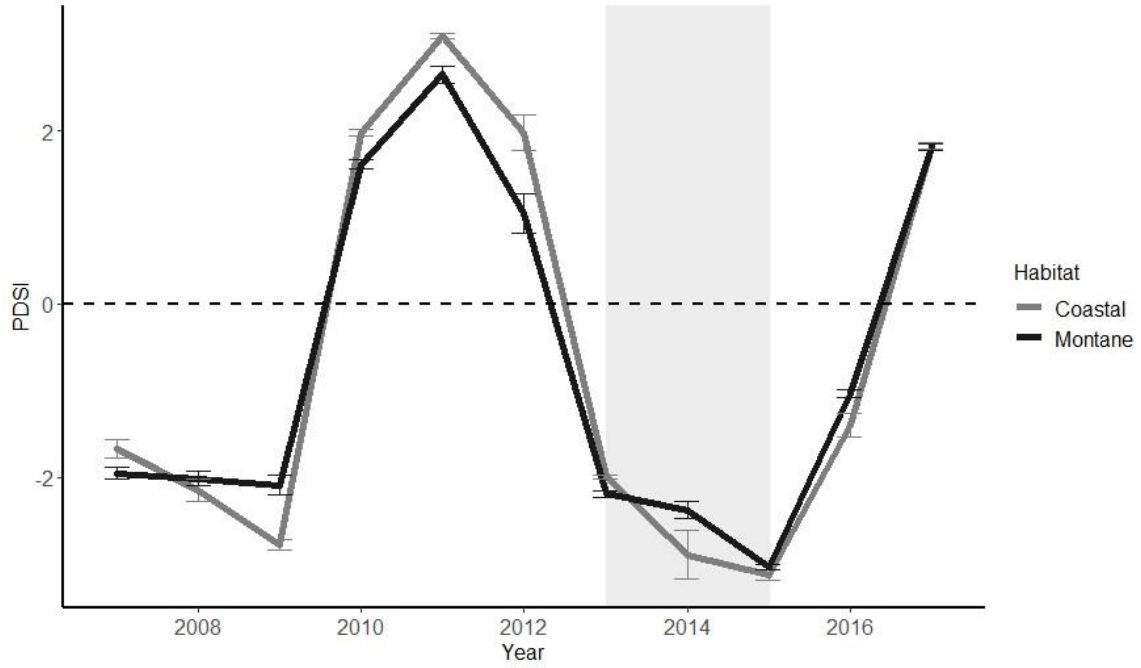

Figure 2. Mean (± SE) Palmer Drought Severity Index (PDSI) values across all study sites (n = 54) in 2007-2017. Study sites are divided into coastal (n = 18) and montane (n = 36) categories. The investigated drought period (PDSI values $\leq$ 2; 2013-2015) for this study is shaded grey.

2.4 Lab Methods

Cores

The dead tree cores were mounted and sanded on a belt sander, with up to 600 grit paper. They were then scanned at 2400 dpi (dots per inch) into the Windendro program (Régent Instruments Inc., Québec, Canada) for measurement following the Dendroecology Lab procedure (K. Watson, pers. comm.). Cores too broken or decayed to dependably measure were not scanned. If rings were difficult to discern from the scanned image, a binocular dissecting microscope was used for cross-referencing. Once the tree-ring series were created, the tree's death date was established through cross-dating

procedures using COFECHA (Holmes, 1984) and live trees that had already been cross-dated for the complementary study. Only cores confidently cross dated using COFECHA and/or qualitatively using marker years (Speer, 2010, p. 2) were included in the analysis.

Basal Disks

To age regeneration, the collected basal disks were sanded down to the root-shoot interface using a belt-sander or hand sanding (up to 1,000 grit), and the interface was identified as the transition zone from pith in the shoot to no pith in the root (Telewski, 1993). Jewelry head lenses, compound microscopes, and binocular dissecting microscope were used throughout the process to ensure the transition zone was accurately identified. The rings at this interface cross-section were counted underneath a binocular dissecting microscope by at least two people to ensure accuracy.

Competition Data

This study aimed to examine the influences of stand density and canopy closure on mortality quantities. Quadratic mean diameter (QMD), a representation of the central tendency of tree diameters that gives more weight to larger trees, and canopy closure (CanClos), a measure of the percent of forest floor covered by canopy, were determined to be appropriate predictors. Additionally, trees per 0.25 ha was used as an exposure variable (see below). Trees per ha (TPH) and QMD were calculated using measurements of DBH (cm) recorded for all live trees within the 0.1 ha subplot and for all dead overstory trees within the 0.25 ha plot. TPH was calculated by multiplying the number of

live trees in the 0.1 ha by 10 to extrapolate per ha. Professional judgment at the sites was used to ensure that the 0.1 ha plot was representative of the ha it was located in. Basal area (BA, m^2) was calculated separately for live trees, dead decay class 1, and dead decay class 2-5 trees to calculate QMD (cm) using the following equation (1) (Erdle, n.d.):

$$BA_i = \sum_{j}^{n} \left(\frac{\pi * DBH_j^2}{40000} \right) \quad (1)$$

BA for live trees was multiplied by 10 and BA for dead trees was multiplied by 4 to extrapolate plot measurements per ha. For models evaluating decay classes, we used one of the following approaches to calculate QMD for each site: 1) The sum of the BA and TPH from live trees and decay class 1 (dead) trees; or, for models evaluating decay class 2-5 trees, 2) the sum of the BA and TPH of live trees and decay class 1-5 (dead) trees. To calculate each site's QMD, the following equation was used (Curtis and Marshall, 2000):

$$QMD = \sqrt{\frac{BA}{.0000785 * TPH}} \quad (2)$$

Exposure Variable

To account for the influence site carrying capacity had on presence of dead trees, the response variable was modeled as a rate of mortality per unit of exposure (TPH). An exposure, when used as a model offset, normalizes the response variable. Thus, the model estimates the effect of predictor variables on the rate of mortality (i.e., a proportion of the dead tree count divided by the estimated tree count prior to death) (Knudsen, 1992). Dead

TPH, used in the calculation for the exposures, was calculated by multiplying the count in the 0.25 ha plot by four. The exposure for models evaluating decay class 1 (DC1) trees was:

$$DC1\ exposure = (\frac{Live\ TPH + DC1\ TPH}{4}) \quad (3)$$

Thus, the exposure for DC1 models was limited to recently live and currently live overstory trees, and was divided by 4 to scale to 0.25 ha for consistency with the response variable. Similarly, the equation for the exposure for decay class 2-5 (DC25) was:

$$DC25\ exposure = (\frac{Live\ TPH + DC1\ TPH + DC25\ TPH}{4}) \quad (4)$$

Drought and Climate Data

To characterize each site's long-term climate, site-specific 30-year (1990-2020) means were calculated for annual precipitation (PPT_{30}) and annual maximum temperature ($T_{max,30}$). Mean annual climatic water deficit (CWD) values for each environment (coastal and montane) were used to evaluate climate influences on mortality and regeneration. All climate data were obtained as monthly values from the TerraClimate database (http://www.climatologylab.org/terraclimate.html) using the coordinates from plot center, then averaged to get annual values. All data were obtained at a 4 km resolution.

Site Characteristics

Each site's elevation and topographic position index (TPI) were used to account for differences in processes such as hydrological balances and cold air drainages (Weiss,

2001). Elevation data were obtained from the USGS National Elevation Dataset program (https://viewer.nationalmap.gov/basic/). TPI compares the elevation of a cell in a digital elevation model (DEM) to the mean elevation of a surrounding neighborhood. Positive TPIs are associated with upper slope positions, zeroes with plains, constant slopes, or saddles, and negative values with lower slope positions or valleys (Weiss, 2001). TPI values were obtained using the *spatialEco* R package (Entekhabi et al., 2022) with a neighborhood (Rodman et al., 2020) representing approximately a 0.5 ha area, with the 0.25 ha plot in the middle.

2.5 Statistical Analysis

Mortality and Regeneration Across Competitive and Habitat Gradients Before and After Drought

Quantities of mortality and regeneration were analyzed through ridge regression with *glmnet* (Friedman et al., 2010) separately for coastal and montane environments due to distinctions in species distributions and climate. When possible, models were further separated by time period: drought/post-drought period verse pre-drought period. Further, death dates were examined by decay class and establishment dates were compared between seedling/sapling size classes.

It was assumed that the counts of mortality and regeneration came from a Poisson distribution and would be modeled with a log link function. The ratio between sample

size and independent variables, termed “events-per-variable” (EPV), was below 10 due to the sample size (coastal n = 18 sites, montane n = 36 sites) and the number of predictor variables for mortality (elevation, CanClos, QMD, TPI, PPT_{30}, $T_{max,30}$) and regeneration (elevation, ground cover, CanClos, TPH, PPT_{30}, TPI, $T_{max,30}$) analyses (Appendix A). Consequentially, variable selection was not appropriate and ridge regression was instead selected. Ridge regression uses a penalty to shrink the coefficient magnitude towards zero, allowing for stabilized estimations of predictor coefficients (Heinze et al., 2018). Specifically, ridge regression is a form of penalized regression, like lasso, based on the L2-penalization of coefficient magnitude (Friedman et al., 2010). Through providing stable solutions, ridge regression improves upon ordinary least squares for models with low EPVs (Blackburn et al., 2021; Heinze et al., 2018).

Prior to running the ridge regressions, several assumptions were evaluated. For the mortality analysis, elevation was log transformed to improve linearity. Additionally, no spatial autocorrelation was found (Moran’s I; *ape* and *geosphere*) (Paradis, 2022). While ridge regression is robust against some assumptions such as overdispersion, variance inflation factors (VIFs) were checked and no predictors were colinear (VIF $\leq$ 3.5). A Poisson distribution was selected that had a lower root mean squared error (RMSE) compared to negative binomial families. RMSE is a measure of standard deviation of residuals and is expressed in the same units as the response variable. An ideal RMSE for the model is one with a similar value to the “natural” ecological variation (irreducible error) (Blackburn et al., 2021).

All variables were rescaled and standardized prior to running a bootstrap analysis (1,000 trials) to further enable robust analysis for the small sample size (Norazan et al., 2009; Zahari et al., 2014). Prior to running the bootstrap analysis, a penalization or tuning parameter (λ) for each ridge regression model was selected to stabilize, or reduce, model variance by introducing a small amount of bias (i.e., shrunken coefficient estimates) (James et al., 2021). Using all of the data, the magnitude of λ was chosen via cross-validation for each model (Blackburn et al., 2021; Friedman et al., 2010). During the bootstrap analyses of the penalized regressions, all models were trained and tested on equivalent splits, allowing for comparison of errors of the full model and the null model.

As ridge regression includes all the predictors in the final model, significance of variables cannot be determined, nor can the magnitude of coefficients be compared between models. Still, the variables' relative importance within the model can be compared using the relative magnitude of the standardized coefficient estimates. To quantify the improvement in predictive power of the full model compared to the null model, RMSEs from the full model were subtracted from RMSEs of the null model for each trial. Lastly, *R*-squared (R^2) values were calculated using the ridge estimated median coefficient values for each model.

Climatic Water Deficit, Mortality, and Regeneration

To identify the influence of climate on tree mortality and regeneration trends, Superposed Epoch Analysis (SEA) was performed using the R package dplR (Bunn et al., 2016). SEA uses bootstrapped confidence intervals (1,000 trials) to check for significant

departures from the mean for a chosen set of event years along with lagged years (Mariani et al., 2016). Event years were defined as years with 10 or more death or establishment dates and were compared with annual CWD values. For mortality analyses, only trees having died since 2005 were evaluated, as decay reduced the amount of trees successfully dated prior to 2005. To evaluate recent regeneration, excluding germinants, the year range 1980 to 2019 was chosen for SEA.

3. RESULTS

3.1 Drivers of Mortality

After graphically determining that decay class 1 (DC1) trees generally died in the later years of the drought and after the drought (**Error! Reference source not found.**), a Kruskal-Wallis test determined a significant difference in death dates between DC1 trees and decay class two through three trees. As older death dates were associated with more decayed classes, it was concluded that decay class four and five trees (which were not generally datable) also died prior to the drought period. Therefore, the bootstrap and estimation of ridge regression models was repeated for each model: coastal drought-related mortality (DC1 trees), coastal pre-drought mortality (decay class 2-5 trees; DC25 trees), montane drought-related mortality (DC1 trees), and montane pre-drought trees (DC25 trees). Due to a limited number of dated death dates of trees (total $n = 209$, coastal $n = 45$, montane $n = 164$), we combined montane and coastal environments for death dating purposes. The combined analysis was verified with separate environment analyses (Appendix C). Due to these death dates, DC1 and DC25 trees will hereafter be referred to as drought-related and pre-drought mortality respectively.

Figure 3. A) Death years by decay class 1 (*n* = 99, median = 2016, mean = 2016), decay class 2 (*n* = 77, median = 2012, mean = 2010), and decay class 3 (*n* = 33, median = 2009, mean = 2008) and B) death years for decay class 1 and decay class 2 and 3 grouped (*n* = 110, median = 2011, mean = 2009). Drought period (2013-2015) is shaded grey.

The strongest predictor for drought-related mortality was canopy closure in montane environments, and TPI in coastal environment (Figure 4 and Figure 5). QMD had a relatively strong negative relationship with montane drought-related mortality, indicating that as the central tendency of tree size increased the rate of drought-related mortality per total trees decreased. PPT_{30} and $T_{max,30}$ had the largest and second largest (positive) median coefficients for montane pre-drought mortality, respectively. This indicated that montane pre-drought mortality was higher in warmer, wetter sites. Like drought-related mortality, montane pre-drought mortality also had a negative relationship with canopy closure. Coastal sites characterized by higher elevation, larger QMDs, lower

$T_{max,30}$, and lower TPI had lower rates of drought-related mortality (Figure 5). Elevation and $T_{max,30}$ had the largest positive relationships with rates of pre-drought mortality. Thus, unlike drought-related mortality, coastal pre-drought mortality was lower at lower elevations. The models' R^2 values ranged from 0.14 to 0.52, with varying degrees of error (Table 1, Appendix D).

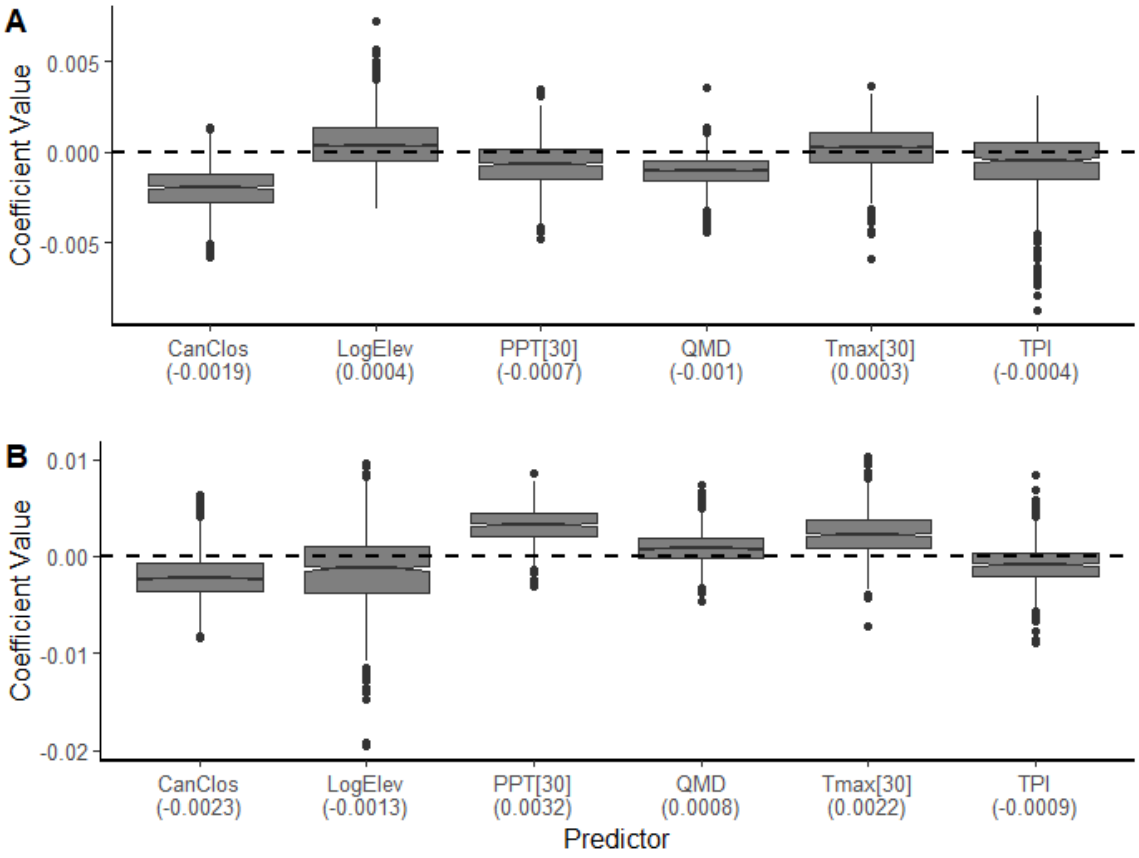

Figure 4. Covariate coefficient distributions from the bootstrap ridge estimation; intercept covariate not included due to scale limitation. A) Montane drought-related mortality (DC1 trees); intercept median coefficient was -2.88 with 95% confidence interval ranging from -3.18 to -2.61. B) Montane pre-drought mortality (DC25 trees); intercept median coefficient was -2.23 with 95% confidence interval ranging from -2.57 to -1.96. Predictor abbreviations include: CanClos (Canopy Closure), LogElev (log of elevation), PPT[30] (30-year mean annual precipitation), QMD (quadratic mean diameter), TMax[30] (30-year mean annual maximum temperature), and TPI (topographic position index). Parenthetical numbers indicate coefficient median values. Note differing vertical axis scales between panels.

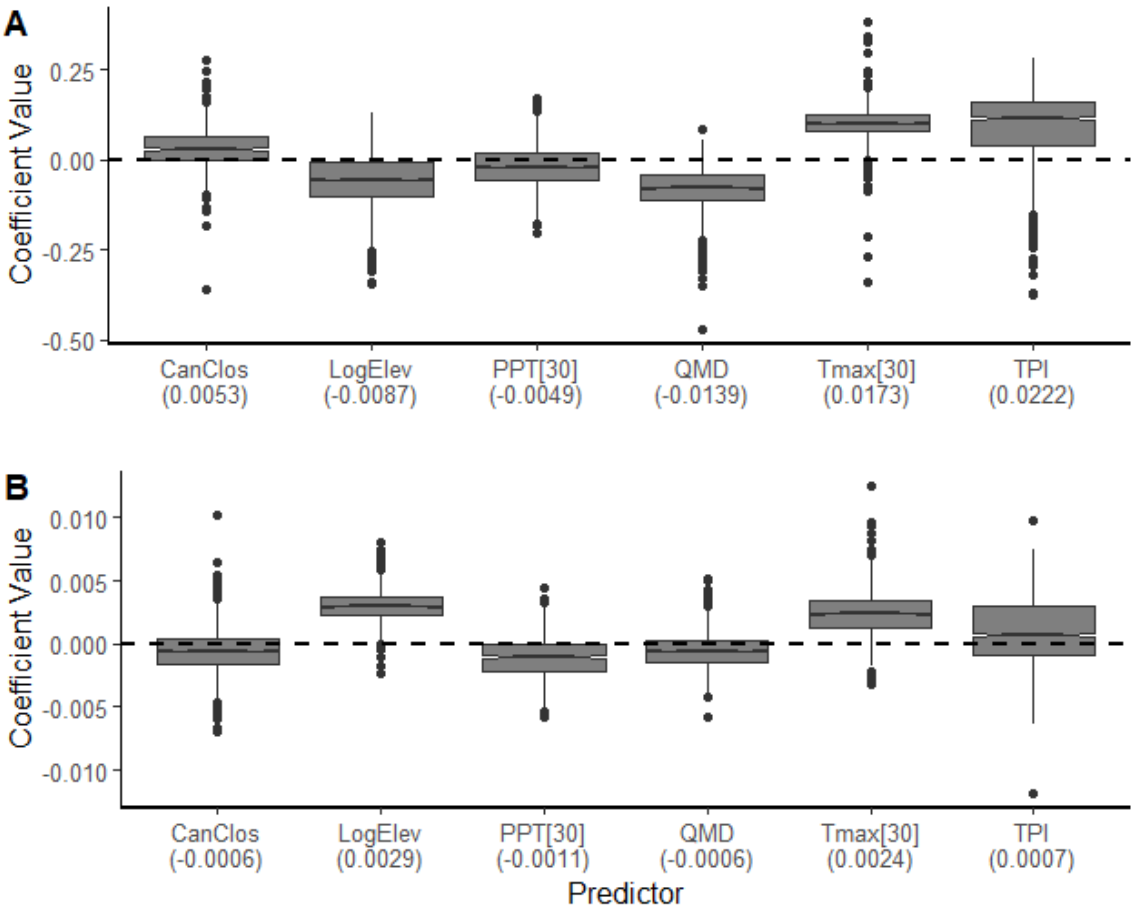

Figure 5. Covariate coefficient distributions from the bootstrap ridge estimation; intercept covariate not included due to scale limitation. A) Coastal drought-related mortality (DC1 trees); intercept median coefficient was -3.43 with 95% confidence interval ranging from -4.04 to -3.05. B) Coastal pre-drought mortality (DC25 trees); intercept median coefficient was -1.86 with 95% confidence interval ranging from -2.10 to -1.69. Predictor abbreviations include: CanClos (Canopy Closure), LogElev (log of elevation), PPT[30] (30-year mean annual precipitation), QMD (quadratic mean diameter), TMax[30] (30-year mean annual maximum temperature), and TPI (topographic position index). Parenthetical numbers indicate coefficient median values. Note differing vertical axis scales between panels.

Table 1. Descriptive statistics for the four models predicting rate of montane drought-related mortality (DC1 trees), montane pre-drought mortality (DC25 trees), coastal drought-related mortality (DC1 trees), and coastal pre-drought mortality (DC25 trees). All values, save the R^2, are median values from the ridge bootstrap analysis. The abbreviation RMSE indicates root-mean squared error.

Model	R^2	Response #	Full Model RMSE	RMSE Difference (Null - Full)
Montane Drought-related Mortality	0.28	4.0	6.0	1.8
Montane Pre-drought Mortality	0.14	11.5	13.3	2.5
Coastal Drought-related Mortality	0.29	1.0	2.2	0.4
Coastal Pre-drought Mortality	0.52	10.0	5.6	3.0

When all decay classes were pooled, no significant difference was found between montane (15 ± 1.8 %, n = 36) and coastal (18 ± 1.7%, n = 18) mortality rates (W = 395, p = 0.20, Mann-Whitney test, **Error! Reference source not found.**). In montane environments, the rate of pooled dead trees both had positive relationships with PPT_{30} and $T_{max,30}$ and a negative relationship with canopy closure. In coastal trees, the rate of all dead trees had strong positive relationships with elevation and $T_{max,30}$ and negative relationships with QMD and PPT_{30}. The R^2 for the montane and coastal models predicting total mortality were 0.21 and 0.72, respectively.

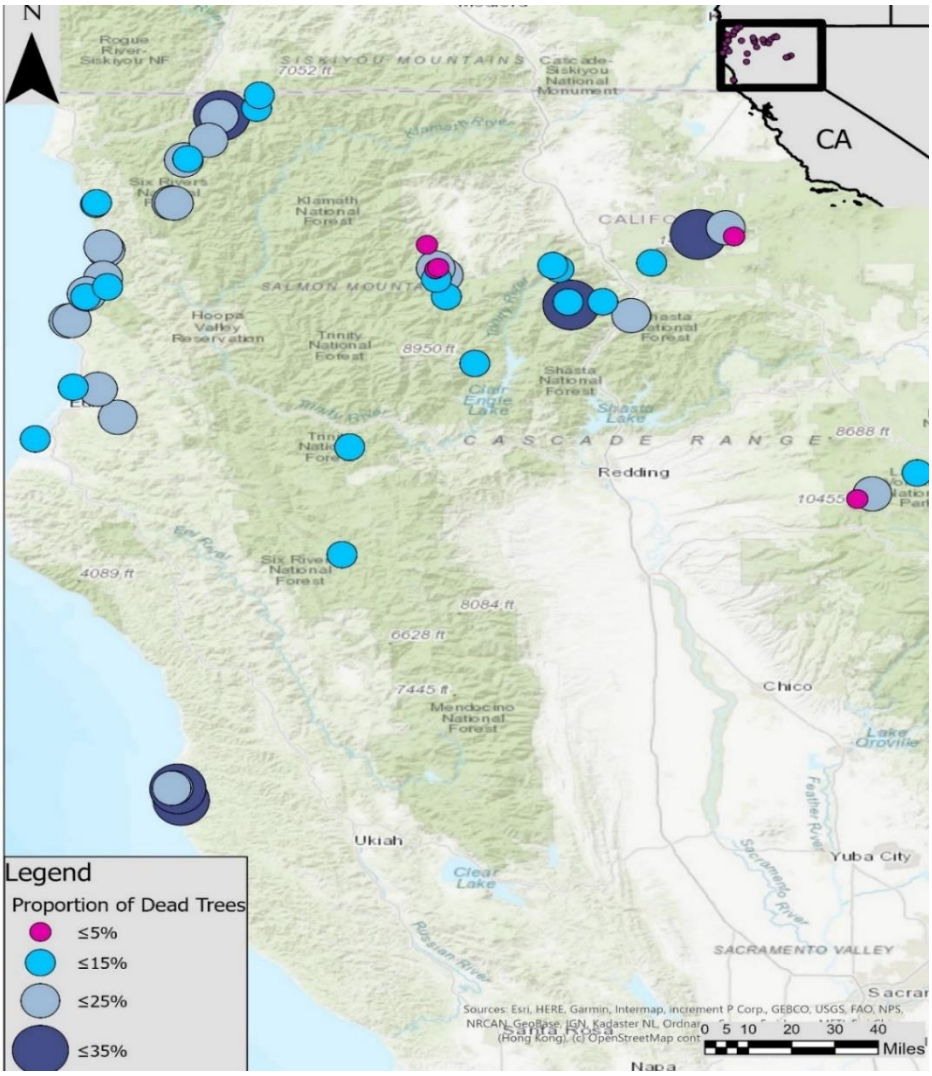

Figure 6. Map of mortality rates by site. Circle symbols represent the locations of study sites, with the size and color of the circle proportional to the percent of dead trees at the plot; larger circles represent increased mortality rates

Overall mortality was more prevalent in *Pinus* sp. compared to other genera, and in smaller diameter trees (Figure 7 and **Error! Reference source not found.**). The highest rates of overstory mortality across all sites were observed in grand fir (*Abies grandis* Douglas ex. D. Don, 51%), sugar pine (43%), and western white pine (37%) (Figure 7). Brewer spruce (6%) and Sitka spruce (9%) had the lowest average mortality

rates. Mortality rates by species and decay classes were not calculated because of an imbalance in dated death years. Drought-related mortality was concentrated in smaller diameter classes, while pre-drought mortality was more evenly distributed among all diameter size classes (**Error! Reference source not found.**). This trend was most pronounced in coastal environments where a sizable portion (16%) of the pre-drought

mortality had trees > 120 cm DBH and no drought-related mortality with trees > 80 cm DBH.

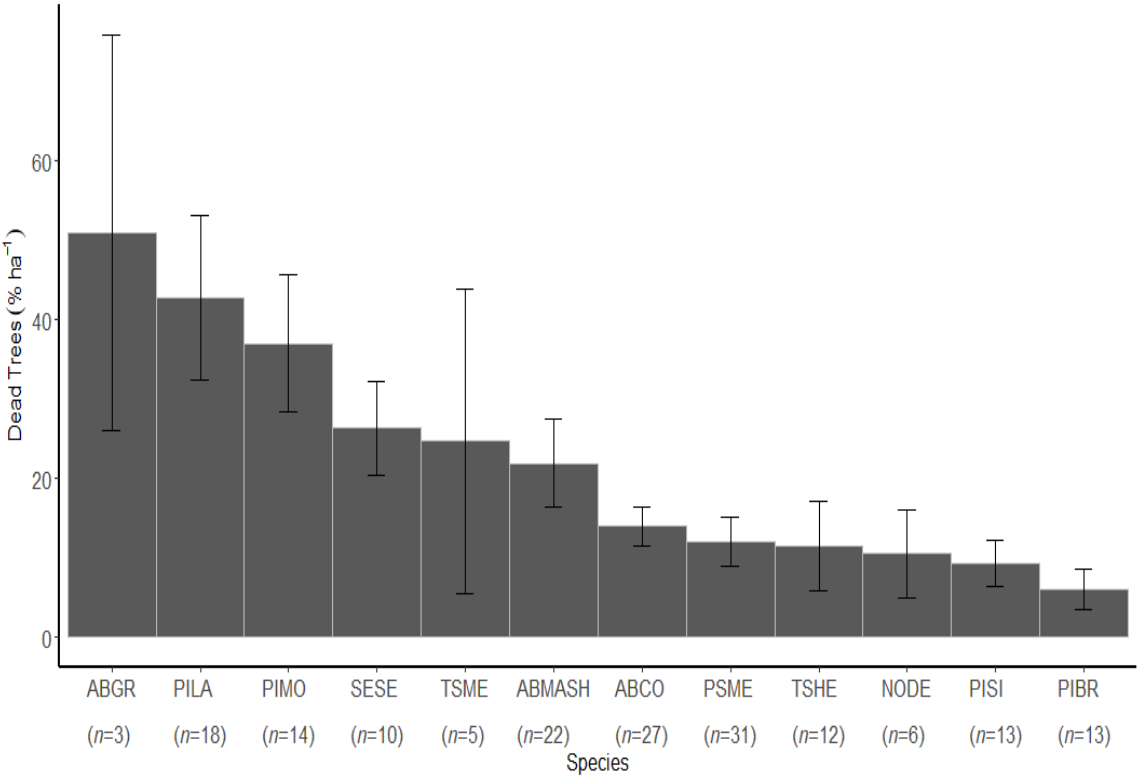

Figure 7. Mean (± SE) percent dead trees per ha for species with $n \geq 60$ across all sites; specific values were calculated across all sites in which that species occurred. Mortality includes both pre-drought and drought-related time periods. Parenthetical numbers indicate the number of sites in which a species occurred. Abbreviations: ABGR (*Abies grandis*), PILA (*Pinus lambertiana*), PIMO (*Pinus monticola*), SESE (*Sequoia sempervirens*), TSME (*Tsuga mertensiana*), ABMASH (*Abies magnifica* var. *shastensis*), ABCO (*Abies concolor*), PSME (*Pseudotsuga menziesii*), TSHE (*Tsuga heterophylla*), NODE (*Notholithocarpus densiflorus*), PISI (*Picea sitchensis*), and PIBR (*Picea breweriana*).

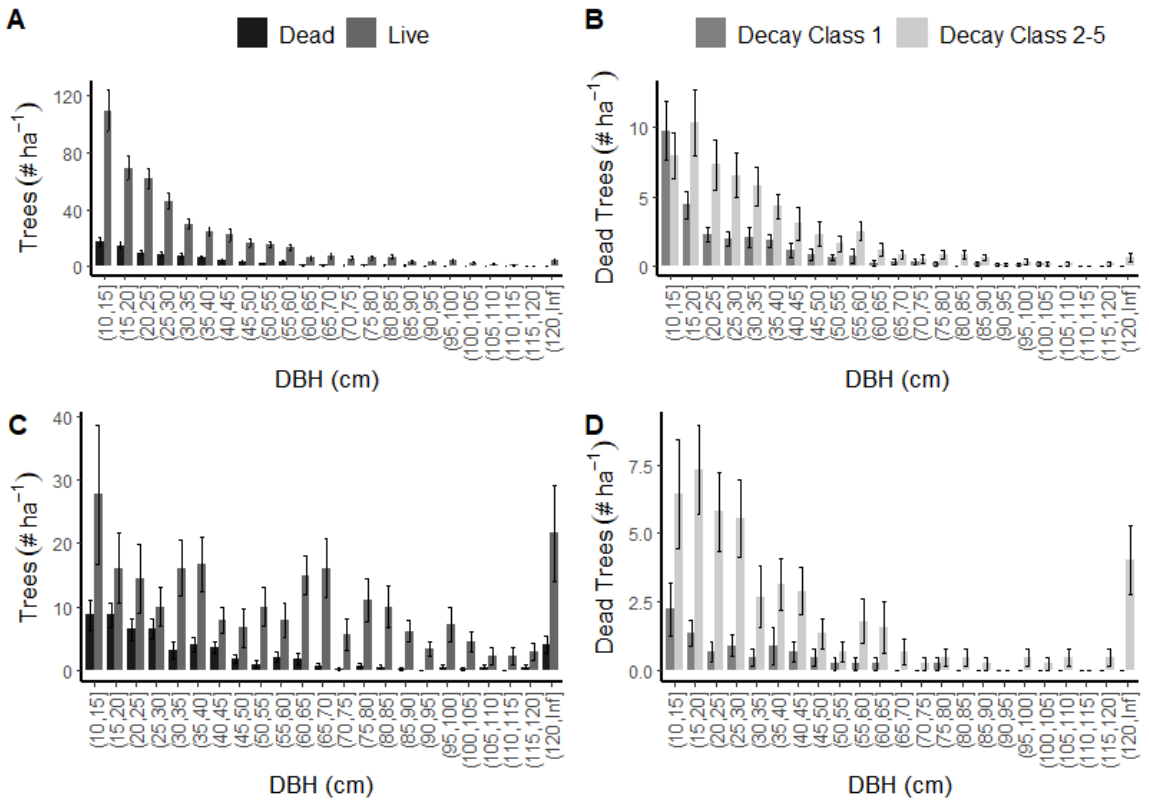

Figure 8. A) Montane number of live and dead overstory trees per hectare by diameter at breast height (DBH). B) Montane number of dead overstory trees per hectare by DBH and decay class. C) Coastal number of live and dead overstory trees per hectare by DBH. D) Coastal number of dead overstory trees by DBH and decay class. All columns are mean (± SE) values based on pre-drought and drought-related time periods. Note the differing scales on y axes.

3.3 Drivers of Regeneration

To determine if regeneration trends differed before and during/after the drought period, differences between seedling and sapling establishment dates were evaluated. The smallest seedings (e.g., seedling I) tended to have more recent establishment dates (Figure 9**Error! Reference source not found.**). Note that sapling IIs were difficult to remove from forest floor, accordingly only one was sampled (established in 1991).

Nearly all regeneration established before the drought period. Thus, seedlings and saplings were pooled, as both groups represented pre-drought regeneration.

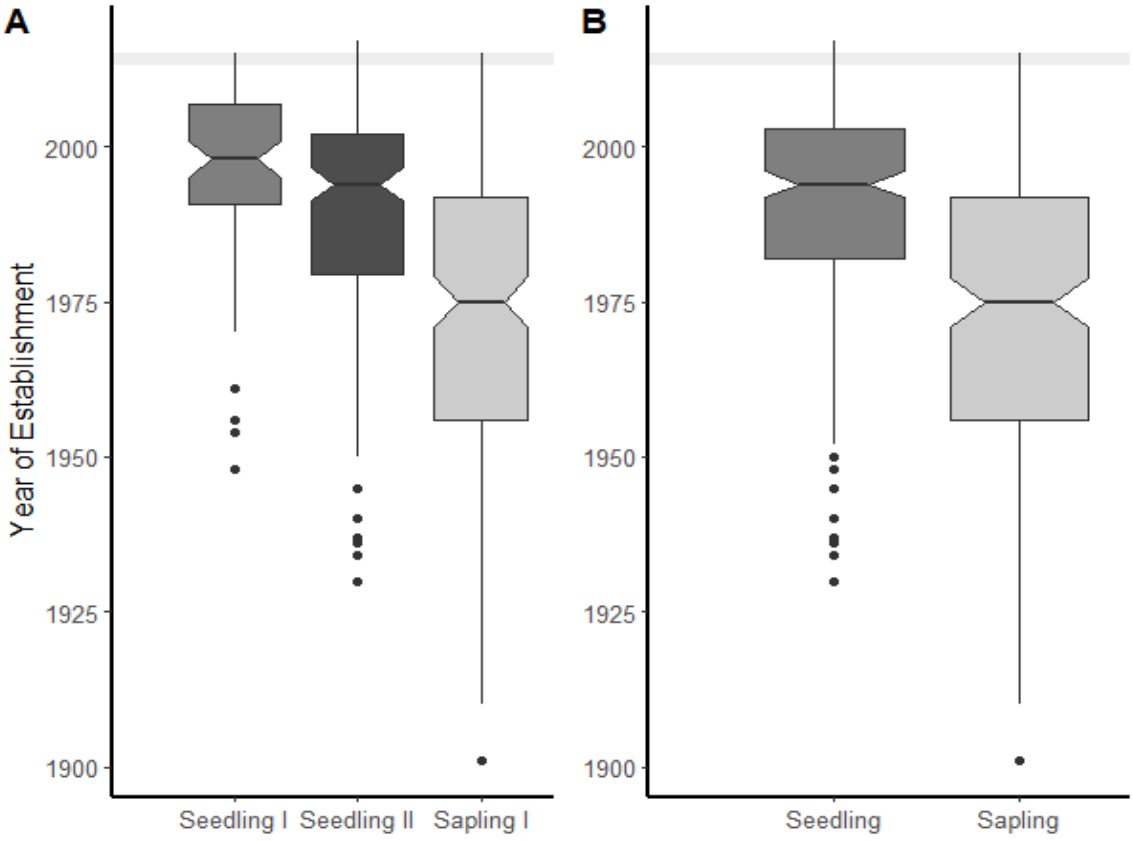

Figure 9. A) Establishment years by regeneration category; seedling I (n = 76, median =1998, mean = 1995), seedling II (n = 183, median = 1994, mean = 1989), sapling I (n = 201, median = 19991 mean = 1991). Only one sapling II was dated, establishing in 1991. B) Regeneration years for grouped seedlings (n = 259, median = 1994, mean = 1991) and grouped saplings (n = 202, median = 1975, mean = 1973). Drought period (2013-2015) is shaded grey.

In both montane and coastal environments, the strongest (positive) predictor of regeneration was TPH (**Error! Reference source not found.**). Regeneration in montane environments was also positively related to $T_{max,30}$, canopy closure, and TPI, in descending order of strength. However, the model's overall R^2 value was only 0.05. In

coastal environments, TPH was followed as the strongest predictor of regeneration by TPI, and $T_{max,30}$, all with positive effects on regeneration. However, unlike montane environments, coastal regeneration was negatively associated with canopy closure. The coastal model described approximately 66% of the variation with varying degrees of error (**Error! Reference source not found.**, Appendix D).

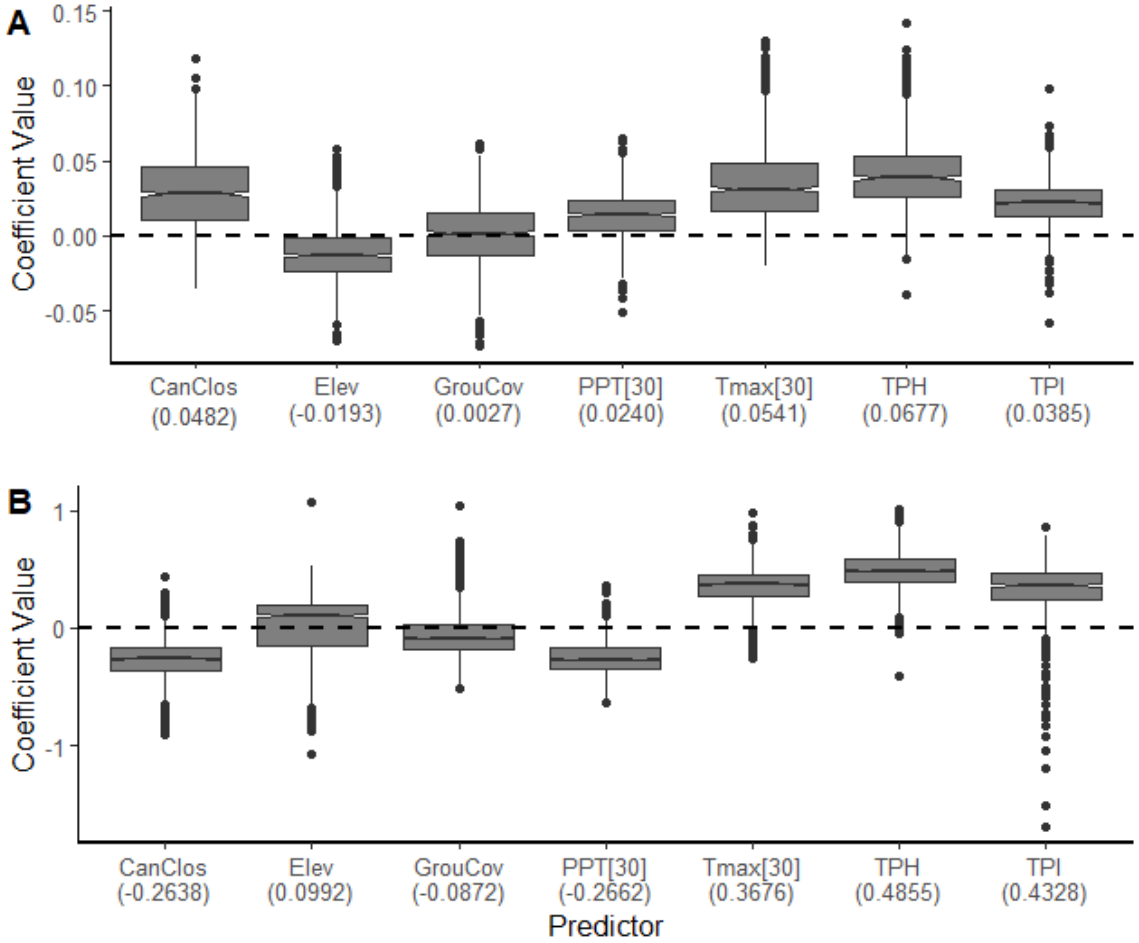

Figure 10. Covariate coefficient distributions from the bootstrap ridge estimation; intercept coefficient not included due to scale limitation. A) Montane regeneration quantities (seedlings and saplings); intercept median coefficient was 4.71 with 95% confidence interval ranging from 4.38 to 5.00. B) Coastal regeneration quantities (seedlings and saplings); intercept median coefficient was 3.60 with 95% confidence interval ranging from 3.07 to 4.03. Predictor abbreviations include: CanClos (Canopy Closure), Elev (elevation), PPT[30] (30-year mean annual precipitation), TMax[30] (30-year mean annual maximum temperature), TPH (live trees per hectare), and TPI (topographic position index). Parenthetical numbers indicate coefficient median values. Note differing vertical axis scales between panels.

Table 2. Descriptive statistics for the two models predicting the quantity of regeneration (seedling and saplings) in montane and coastal environments. All values, save the R^2, are median values from the ridge bootstrap analysis. The abbreviation RMSE indicates root-mean squared error.

Model	R^2	Response #	Full Model RMSE	RMSE Difference (Null - Full)
Montane	5%	100.5	85.43	0.85
Coastal	67%	29.50	51.03	11.33

Overall, there was less regeneration in coastal environments compared to montane environments. In both environments, shade-tolerant species, namely true firs, outnumbered shade-intolerant species (Figure 11 and Figure 12**Error! Reference source not found.**). In montane environments, shade-tolerant white fir, Shasta red fir, and mountain hemlock were the most common regeneration species. Brewer spruce was more commonly found as a sapling than a seedling. In montane environments less than half the number of white pines (sugar pine and western white pine) occurred than true firs. In coastal environments, the most common sapling species was tanoak (*Notholithocarpus* densiflorus (Hook & Arn) Manos, Cannon & S.H.Oh) and the most common seedling was grand fir. Hardwood and shade-intolerant seedling species were found at similar rates in coastal environments.

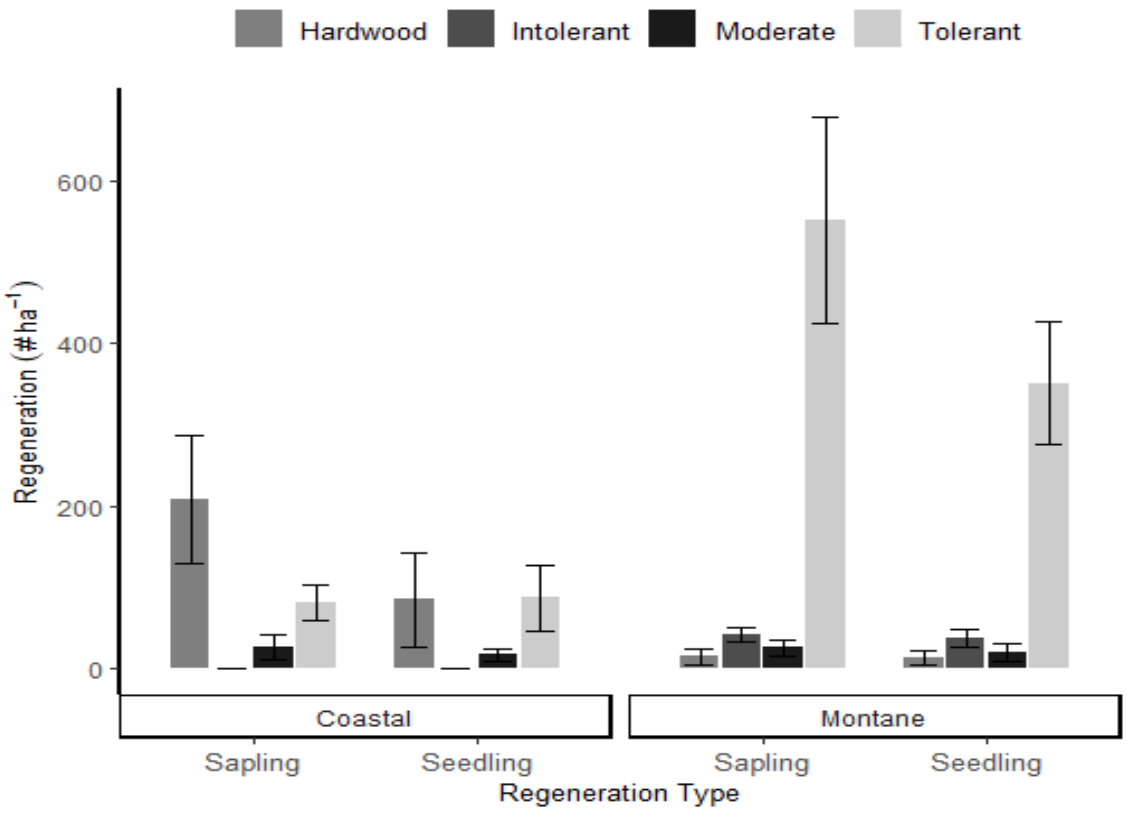

Figure 11. Mean (± SE) number of hardwoods, shade-intolerant, moderately shade-tolerant, and shade-tolerant seedlings and saplings per hectare in coastal and montane environments.

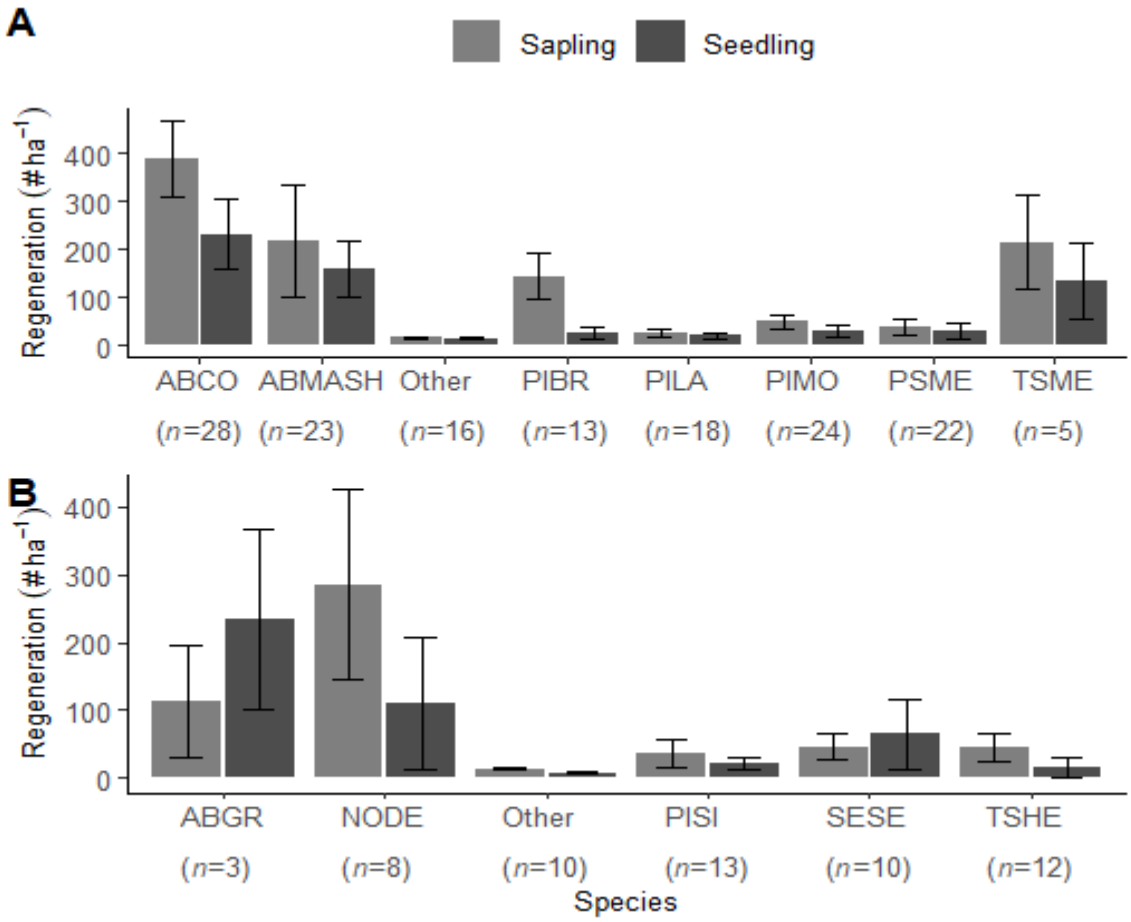

Figure 12. Mean (± SE) number of seedlings and saplings present per hectare by species for A) montane environments and B) coastal environments. Parenthetical numbers indicate the number of sites in which a species occurred. Abbreviations: ABCO (*Abies concolor*), ABGR (*Abies grandis*), ABMASH (*Abies magnifica* var. *shastensis*), NODE (*Notholithocarpus densiflorus*), PIBR (*Picea breweriana*), PILA (*Pinus lambertiana*), PISI (*Picea sitchensis*), PSME (*Pseudotsuga menziesii*), SESE (*Sequoia sempervirens*), TSHE (*Tsuga heterophylla*), and TSME (*Tsuga mertensiana*). The "Other" categories include *Alnus* spp., *Pinus attenuata*, *Pinus contorta* ssp. *contorta*, *Pinus contorta* ssp. *murrayana*, and *Quercus* spp., along with a few unidentified hardwoods. Note that only plots which had the presence of the pertaining species were considered.

3.4 Climatic Water Deficit, Mortality, and Regeneration Trends

The median death year of dated dead trees was 2014 (range 1987-2020). In both montane and coastal environments, the trendlines showed a similar pattern with a lag

between CWD and tree mortality (**Error! Reference source not found.**). In montane environments, seven years were identified as high mortality years (≥ 10 death dates) between 2005 and 2020: 2013, 2014, 2015, 2016, 2017, 2018, 2019. Along with the spike in mortality in the 2013-2015 drought period, there was also a relatively smaller spike of mortality during the 2007-2009 drought (which also had PDSI values ≤ -2; **Error! Reference source not found.**). Mortality events in montane environments had a significant ($p < 0.05$) positive relationship with CWD during the death year and one and two years preceding the death year (Appendix FAppendix F). In coastal environments there were no years between 2005 and 2020 with 10 death dates for analysis.

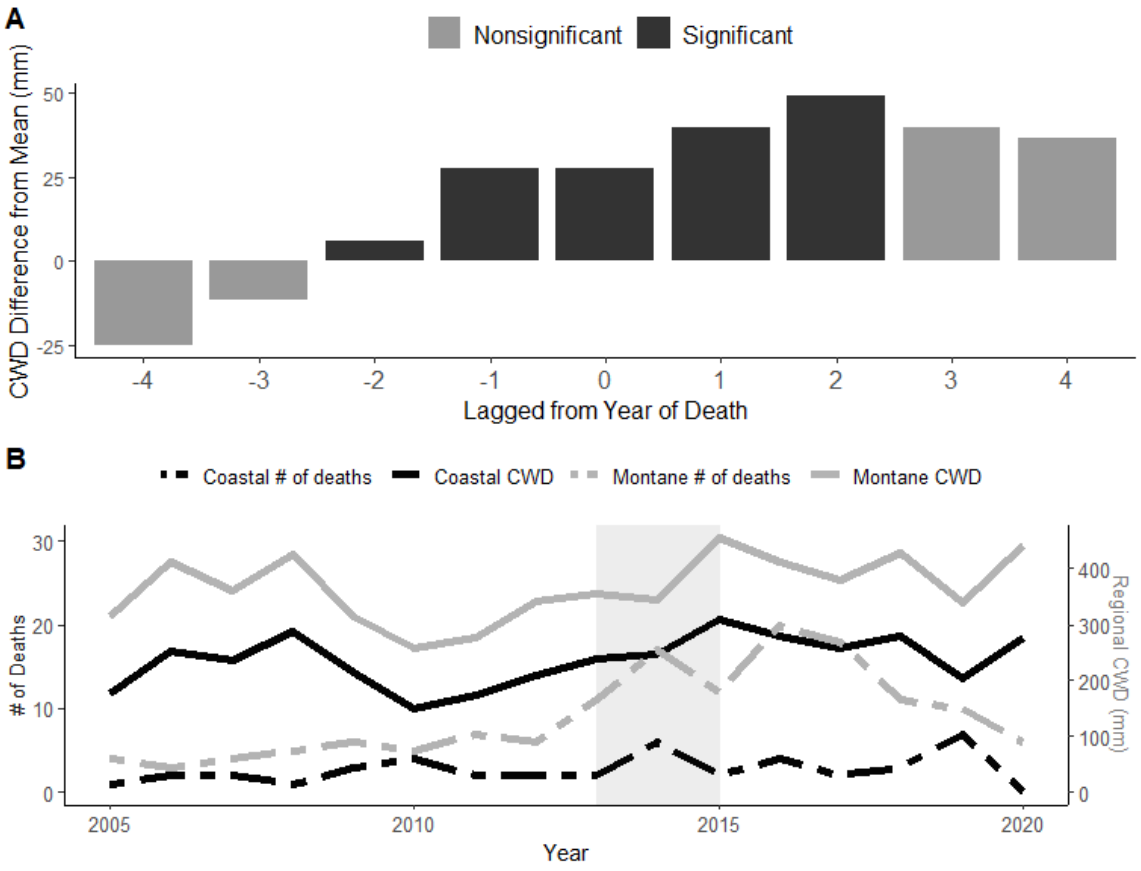

Figure 13. A) Montane superposed epoch analysis (SEA) results showing climatic water deficit (CWD) departures from the mean CWD (2005-2020) for years of high mortality. Dark bars indicate lags with a significant CWD departure ($p < 0.05$) from the mean. B) Annual number of dated dead trees and regional annual CWD for coastal and montane environments. The smaller number of dead coastal trees is in part due to the fact coastal cores were more decayed and therefore difficult to date. The vertical gray bar indicates the drought period. Note: Coastal SEA was not possible due to an insufficient sample size of event years.

The median height of dated regeneration was 28 cm and the median establishment year was 1988 (range 1901-2017; Figure 14). In montane environments, eight years were high event years ($\geq$ 10 establishment dates) between 1980 and 2019: 1986, 1987, 1990, 1994, 1996, 1998, 1999, and 2002. Montane environments had a signficant negative relationship with CWD in the year preceding regeneration events (Figure 15, Appendix

F). In coastal environments, only one year (2011) had over 10 dated regenerations; this sample size was inadequate for SEA. After the drought period, no regeneration established in montane enviroments, and only one established in coastal environments. In both environments, a lagged increase in establishment was evident following years with relatively low CWD.

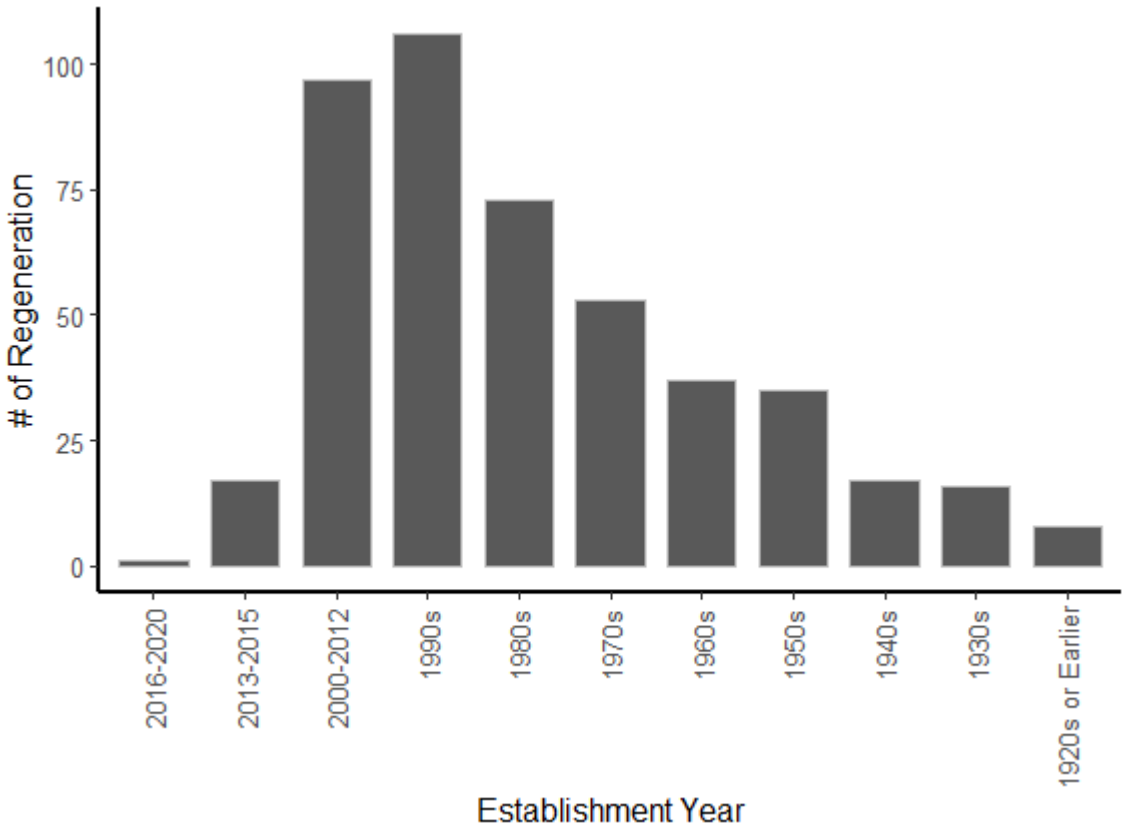

Figure 14. Quantity of dated regeneration samples established in each decade, during the 2013-2015 drought, and the post-drought period. Note that the time period bins are not equivalent for the most recent bins compared to prior decades. Quantities are for pooled montane and coastal environments.

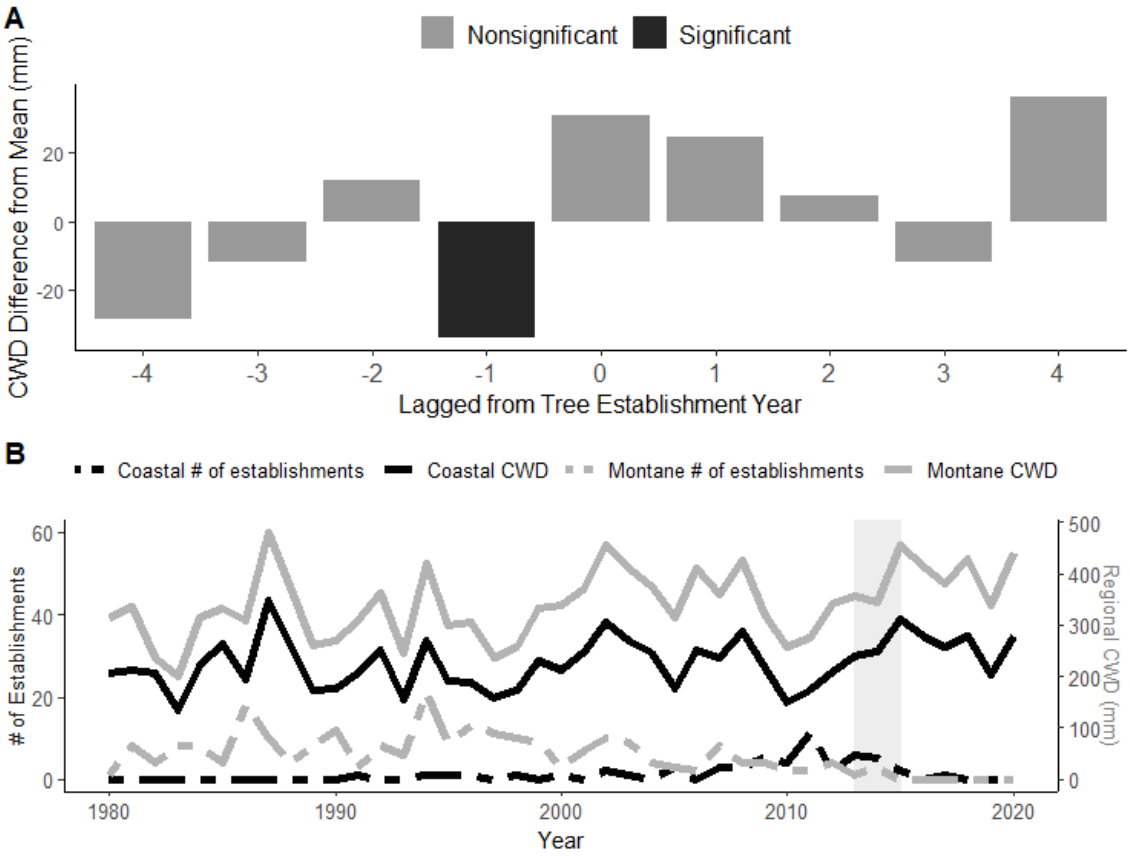

Figure 15. A) Montane superposed epoch analysis (SEA) results showing climatic water deficit (CWD) values for years of high regeneration establishment; dark bars indicate lags with a significant CWD departure ($p < 0.05$) from the mean (red dashed line, 1980-2019). B) Annual number of dated established regeneration and annual CWD for coastal and montane environments. The vertical gray bar indicates the drought period. Note: Coastal SEA was not possible due to an insufficient sample size of event years.

4. DISCUSSION

This work found meaningful trends between forest demographics and drought in northern California. Mortality and regeneration patterns varied before and during/after the drought period and between coastal and montane environments. Montane drought-related mortality occurred in sites with more canopy openness and was highest in white pine species; coastal drought-related mortality was highest in warm sites with high topographic position indices. In both montane and coastal environments, drought-related mortality was concentrated in smaller trees. Regeneration in both environments was weighted towards older (20+ years) shade-tolerant species, with few shade-intolerants present. These findings suggest that management efforts to enhance drought resistance and diversity should target montane stands containing white pines and coastal sites with warmer temperatures and greater exposures (i.e., high TPI values). Additionally, because small trees in this region were more prone to drought-related mortality, preferential retention of medium and large trees will likely increase forest resistance and resilience. Our observations of high white pine mortality coupled with low white pine regeneration indicate that artificial regeneration efforts (e.g., planting seeds or seedlings) should favor these taxa, if they are to persist in these landscapes. Lastly, creating and allowing more disturbances (e.g., gaps, prescribed fires, wildfires) will foster a diverse and younger understory.

4.1 Drivers of Mortality

Montane Environments

A primary difference between drought-related montane mortality and pre-drought mortality was that pre-drought mortality had a positive relationship with mean precipitation (PPT_{30}), while drought-related mortality had a relatively weak negative relationship with precipitation. Prior studies have demonstrated that as drought severity increases, drier stands with higher mean CWD have higher mortality (Young et al., 2017). We found a similar trend of drought-related mortality and a negative relationship with mean precipitation, which was not found for pre-drought mortality. Pre-drought mortality may have been more related to pathogens, such as white pine blister rust (*Cronartium ribicola* J.C.Fisch in Rabh), that thrive in moist conditions (National Biological Information Infrastructure and Invasive Species Specialist, 2005; Schwandt et al., 2013), or due to specific acclimations. For example, sugar pine and western white pine, which predominantly died prior to the drought (90% of their mortality), are notably vulnerable to white pine blister rust and hydraulic failure (Martínez-Vilalta et al., 2004). Despite this vulnerability, these pines do not appear to increase stomatal regulation during water stress (Robinson, 2021), amplifying their vulnerability to hydraulic failure. White pines in wetter sites were likely acclimated to ample water availability and vulnerable to drought (including periods of water stress prior to the 2013-2015 drought). through hydraulic failure and/or decreased defense mechanisms. Specifically, sugar pine

and western white pine overall mortality rates (decay classes 1-5) had a significant positive relationship with mean precipitation (Appendix G).

In montane environments, more open canopy sites had a higher rate of mortality, particularly drought-related mortality. To contextualize this relationship, very few (4 out of 54) sites had basal areas below 30 m^2 ha^{-1}, a density classified as intermediate to dense in prior studies (Young et al., 2017), and the sites had high trees per ha (median 490 per ha). However, despite the narrow range of densities, montane sites had a wide range of canopy closures (~37-98%), likely enabling the detection of this negative trend between drought-related mortality and canopy closure. This trend was not observed in coastal sites, possibly due to relatively narrow range of canopy closures (~81-99%). A reduction in canopy closure can impact forests via: (1) decreased overstory transpiration coupled with increased understory transpiration, (2) decreased canopy interception of precipitation inputs, (3) increased solar radiation, and (4) increased wind energy (Adams et al., 2012; Anderegg et al., 2013). The net change in soil moisture is not always clear, as reductions in overstory transpiration and interception increase soil moisture, while solar radiation and wind can increase soil temperature and offset some of the moisture gain (Anderegg et al., 2013). Increased wind and more "edges" can also assist in the spread of aerially dispersed pathogens, like white pine blister rust (Kimmey and Wagener, 1961), that can synergize with any reduction in water availability. Although extensive tree mortality typically increases water availability, in drier sites, water yield can decrease following tree mortality (Adams et al., 2012). Our findings of higher drought related mortality in dry sites support this, indicating lower canopy cover likely

translated to increased overstory water stress, causing greater tree mortality. This could be due to greater solar radiation, wind, and understory transpiration.

Coastal Environments

An important difference between coastal drought-related and pre-drought mortality was elevation, with pre-drought mortality having a positive relationship with elevation, and drought-related mortality having a relatively weaker negative relationship. The elevational trends could relate to summer fog, which is most prevalent immediately along the coast (Wilson & Jetz, n.d.) (Grantham, 2018). There can be substantial differences in summer cloud cover between neighboring coastal sites like Arcata (elevation 32 m) and Kneeland (elevation 487 m) (Wilson and Jetz, n.d.), with Kneeland being only 14 km inland from Arcata. Fog cover, including summer fog, has decreased 33% since the early 20th century (Johnstone and Dawson, 2010). Thus, pre-drought trees at lower elevations likely had more cloud cover, ameliorating heat-related stress (Emery et al., 2018), and leading to less mortality than higher elevations. It is also possible that this trend of reduced mortality at lower elevations was partially driven by fast decomposition rates in consistently moist, low-elevation coastal environments (Zanne et al., 2015). Coastal drought-related mortality's contrastingly negative relationship with elevation may be because low-elevation coastal trees were more acclimated to wet conditions caused by the fog and therefore more sensitive to drought, especially given the reductions in summer fog (Johnstone and Dawson, 2010).

Unlike montane environments, mean maximum temperature ($T_{max,30}$) and topographic position index were relatively strong positive predictors of coastal mortality in both time periods, especially recent drought-related mortality. This could be attributable to greater drought sensitivity in coastal species compared to montane species (Robinson, 2021), such that high mean maximum temperature and topographic position index substantially amplified drought conditions.

Tree Size and Mortality

Mortality was higher in smaller diameter classes, and drought-related mortality was higher in stands with lower quadratic mean diameters in both environments. At coastal sites, ~33% of drought-related dead trees were 20 cm DBH or smaller. This trend is contrary to the Sierra Nevada, where drought-related mortality was concentrated in medium to large co-dominant and dominant trees (Das et al., 2016; Stephens et al., 2018; Young et al., 2020). Bark beetles (*Dendroctonus*, *Ips*, and *Scolytus* spp. Erichson), which particularly affect large trees (Das et al., 2016), were more pervasive in the central and southern Sierra Nevada than in northern California (California Forest Pest Council, 2016). Smaller diameter trees, on the other hand, fall victim to suppression-related mortality more frequently than larger diameter trees, particularly trees under 50 cm DBH (Das et al., 2016). Suppression or stem exclusion was likely one of the interacting agents of mortality. Additionally, understory plants, including small trees, typically have shallow roots with presumably limited access to reliable water (Bond et al., 2008; Stubblefield and Reddy, 2021). As young trees grow, transpiration rates exponentially

increase, before slowing down, and ultimately reaching an asymptotic maximum (Bond et al., 2008). Small trees may have had higher water demands for their relatively less developed root systems that contributes to water stress and mortality. Further, insect and pathogens follow on small trees already experiencing suppression and water stress, and can contribute to their mortality (Furniss, 1977). Mortality in montane trees was more balanced across size classes for both pre-drought and drought-related mortality than coastal trees (**Error! Reference source not found.**). This could result from greater insect damage in montane trees, as approximately 25% of montane trees showed signs of potential insect damage compared to only 17% of coastal trees.

The relatively low range of R^2 values (0.14 to 0.52) indicates that while our models explained some of the variation in mortality rates between time periods and environments, there are additional factors at play. One of the largest contributions to Sierra Nevada tree mortality during the recent drought was forest insects and pathogen distribution (Das et al., 2016), which was not modeled in this investigation. Likewise, soil and geologic conditions, known to influence tree mortality (Soong et al., 2020), were not analyzed. Thus, this study provides information about above-ground abiotic dynamics contributing to mortality that likely interact with insects, pathogens, and soils.

4.2 Drivers of Regeneration

Relatively strong relationships between regeneration and stand density (TPH), mean maximum temperature, and canopy closure were found for both montane and

coastal environments. The positive relationship between tree density and regeneration could be because high density signifies high site productivity with abundant overstory trees producing viable seeds. Furthermore, it is possible that some overstory trees established at a similar time as the regeneration, when stand density was lower, but have been more competitive at growing due to favorable microsites, spacing, or genetic predisposition (Oliver and Larson, 1996). Moist and moderately warm conditions are favorable for photosynthesis and are associated with large seed crops (Keyes and Manso, 2015; Lauder et al., 2019). High mean maximum temperature could represent these favorable or unfavorable conditions for trees. For example, some conifers produce large seed crops when stressed as a "flight" mechanism (Lauder et al., 2019), such that the positive relationship between mean maximum temperature and regeneration might result from stressed overstory trees producing bumper seed crops.

Canopy closure represented the greatest difference between montane and coastal regeneration trends. In montane environments, regeneration increased with canopy closure, and the most prominent species were shade-tolerant *Abies* (white and Shasta fir). Interestingly, regeneration was also predominantly advanced regeneration rather than new recruits (median age 39 years, mean age 44 years). Additionally, while high canopy cover may hinder the release of suppressed regeneration, it can also buffer regeneration from high evaporative demands, enabling shade-tolerant species to survive for decades in a suppressed state. Notably, coastal regeneration had a negative relationship with canopy closure, which was the opposite of our findings for montane environments. Under the high canopy closure (81-99%) of coastal sites (versus 37-98% at montane sites), the

presence of any additional light may aid successful seedling regeneration, even for shade-tolerants (Burns and Honkala, 1990; Fryer, 2008). Finally, to contextualize this difference between montane and coastal regeneration's relationships with predictors, the montane regeneration model was relatively weak ($R^2 = 0.05$), whereas the coastal model was strong ($R^2 = 0.67$).

4.3 Northern California Species Perpetuation

Our montane demographics are consistent with prior findings in the Sierra Nevada that found the highest rates of mortality in *Pinus* (Fettig et al., 2019; Stephenson et al., 2019), and regeneration dominated by shade-tolerant trees such as *Abies* (Young et al., 2020). The decline in white pines (i.e., Sugar pine and western white pine) is likely due to their susceptibility to insects and pathogens (Dudney et al., 2020; Young et al., 2020), including white pine blister rust that was observed at some sites. High density stands, like those of our study sites, predispose pines to *Dendroctonus ponderosae* (Hopkins) attacks (Fettig et al., 2007; Wood et al., 2003; Young et al., 2020). These data indicate that the future distribution of white pines is at risk (i.e., dying disproportionaly with limited regeneration).

The highest coastal mortality rate was in grand fir (51%), but was limited to sites in the most mortality-vulnerable part of our coastal study area (i.e., southern portion of the study area in Mendocino County). These were three of the four coastal sites with the highest mean maximum temperatures, and lowest mean precipitation values (third

through fifth) of all coastal sites. These sites represent the southern-most extension of this species' range (Kauffmann, 2012), so demographic findings about these populations are particularly meaningful, as they can inform about potential future shifts in distribution. Dead grand fir tended to be smaller (DBH 24 ± 2 cm) than their live counterparts (DBH 46 ± 3.5 cm). Smaller grand fir may have had less dependable access to ground water during the drought (Stubblefield and Reddy, 2021), and been further vulnerable to insect damage (observed on approximately 37% of grand fir). Known insects that have contributed to grand fir decline in Mendocino County include the balsam wooly adelgid (*Adelges piceae* Ratzeburg), first detected in the area in 2011 (Jones et al., 2019), and the fir engraver beetle (*Scolytus ventralis* LeConte), which is widespread in low-levels across parts of Mendocino County (California Forest Pest Council, 2020). Grand fir affected by these insects have high levels of *Heterobasidion occidentale* (Otrosina & Garbel), a root-disease that serves as a further predisposing factor (Christopher Lee, pers. comm).

The lowest rates of mortality were found in *Picea*. Evidence of forest insects and pathogens (pers. observation), a primary driver of mortality (Das et al., 2016), were sparse on these species relative to other species. Brewer spruce appeared to maintain relatively even stromatal conductance during the drought (Robinson, 2021), a strategy that proved successful in this case. Brewer spruce was the fourth most abundant sapling (145 ± 48 across 13 sites) in montane enviroments, while Sitka spruce was one of the least common species observed in coastal regeneration.

4.4 Climatic Water Deficit, Mortality, and Regeneration Trends

Mortality

While all drought years and the four years following (2013-2015) had high mortality numbers (≥ 10 deaths), only 2014-2017 had over 12 dated deaths, demonstrating increased mortality after the first year of a multi-year drought, and two years after the drought. This lag may be attributed to tree physiological responses to drought delaying the mortality mechanisms of carbon starvation and hydraulic failure (McDowell et al., 2008). The use of stored carbohydrates to support metabolic functions when photosynthesis is water limited (McDowell et al., 2008) could delay drought-induced mortality. Additionally, mortality due to drought-induced hydraulic failure may be delayed, as trees typically need to experience a roughly 60% loss of hydraulic capacity before dying (Adams et al., 2017; Anderegg et al., 2015; Young et al., 2017). Thus, significantly high CWD in years preceding tree death likely causes gradual carbon depletion and the accumulation of hydraulic damage. Many forest pests such as bark beetles amplify drought effects, and continue attacking weakened trees after drought (Millar and Stephenson, 2015; Young et al., 2017). A combination of these mechanisms (e.g., hydraulic failure, carbon starvation, and/or biotic agents) likely drive tree death (Manion, 1981) and explain the importance of CWD in the preceding years. The limited number of coastal event years is likely related to the fact that cores extracted from dead trees in this consistently wet environment were more crumbly and broken, making them harder to date.

Regeneration

Conifer reproductive cycles, including seed germination, takes multiple years and relatively few seeds successfully germinate and survive to adulthood (Fowells, 1965; Minore, 1986). For some species such as western white pine, seeds can stay viable in the duff for up to four years, with germination rate decreasing over that time period (Griffith, 1992). For white fir, cones are fertilized, reach full size, and begin seed dispersal in autumn the year prior to germination (Zouhar, 2001). For both of these conifer species, the importance of available moisture the year prior to successful germination is clear: it ensures stratification and adequate resources for germination early in the following year.

The age range (3 to 119 years; median of 32 years) of all regeneration suggests limited successful, recent replacement following overstory mortality, with approximately 80% of the regeneration older than 20 years . Further, only one coastal seedling and no montane regeneration established since 2015. This indicates that stand conditions are likely limiting and/or climatic conditions have been inadequate for successful regeneration. Conversely, it is also possible that recent regeneration is occurring, but not detected (i.e., germinants were not counted and/or were browsed). The advanced regeneration throughout the sites indicates slow growth rates in seedlings and saplings, likely due to the shaded environments that characterized most of the coastal and montane regeneration sites (Pirtel et al. 2021). Notably, these study sites lacked recent disturbances such as active management and/or wildfire, which generally create favorable

conditions for shade-intolerant species, and increase growing space and light in the understory to support faster growth rates (Pirtel et al., 2021).

4.5 Management Implications and Future Directions

Northern California is renowned for its diverse and ubiquitous forests and is economically dependent on the forest product industry (i.e., Humboldt, Shasta, and Siskiyou Counties consistently provide most of the state's harvested timber volume; California Department of Tax and Fee Administration 2020). Currently, northern California is experiencing the worst drought severity with the highest acreage of tree mortality across the state (USDA, 2021). Climate-driven tree mortality can increase fuel availability and increase the energy released during wildfire (Goodwin et al., 2021). Thus, learning from past record-setting droughts can inform management in this region to support the sustainment of invaluable biodiversity and forest resources.

These findings can help guide silvicultural prescriptions, such as thinning and prescribed fire, to enhance forest drought resistance, resilience, and stand structure (O'Hara et al., 2012; Soland et al., 2021; Stephens et al., 2020; van Mantgem et al., 2016; Vernon et al., 2018). Some current California Forest Practice Rules include canopy cover language, such as the Forest Fire Prevention Exemption and the Emergency Notice for Fuel Hazard Reduction (14 CCR § 1052.4 and §1038.3), which require a maintenance of at least 30-50% canopy cover depending on the stand type and specific permit. Silviculture prescriptions like Group Selection or Variable Retention, allow for a

diversity of canopy openings (*California Forest Practice Rules*, 2022), and can therefore be tools to balance denser canopy cover maintenance in some areas, while promoting gaps and shade-intolerant species regeneration in other areas. In coastal environments, management aimed at reducing drought-related mortality should be focused on sites with the warmest summers, which are at the southern edge of the study area. In both coastal and montane environments, more drought-related mortality was observed in smaller trees. There was no drought-related mortality on the coast in trees with DBH greater than 80 cm and the majority (~80%) of the montane drought-related mortality occurred in trees smaller than 40 cm DBH. Thus, management should aim to foster landscapes with trees greater than 80 cm DBH on the coast and 40 cm DBH in montane environments, as these trees likely have more developed roots to sustain water use during drought.

The Klamath Mountains of northern California are renowned for biodiversity, hosting over 30 conifer species (Kauffmann, 2012). However, our data show that these forests' relative species abundance is shifting, with the montane regeneration dominated by white fir and Shasta fir. Species like white pines have higher mortality and are limited in the understory. To maximize white pine perpetuation, management prescriptions could prioritize growing space around these species; this will increase resource availability, productivity, and available photosynthate to produce secondary compounds for increased protection against forest pests (Smith et al., 1996). This type of prescription should be prioritized in wetter parts of white pines' range where higher mortality rates were measured. To facilitate regeneration, gaps or group selection units should be

preferentially placed next to mature white pines, so these shade-intolerant species have areas where they are most competitive at regenerating.

The final management implication from our study is that recent successful regeneration appears limited (i.e., we found a median age of seedlings and saplings of 33 years, and approximately 80% of the regeneration older than 20 years), leaving uncertainties regarding forest perpetuation. Canopy openness leads to significantly taller, larger juvenile trees (Pirtel et al., 2021), and more shade-intolerant species. Thus, to encourage more diverse and responsive regeneration, disturbances that foster canopy openings should be promoted, especially in montane environments. While this may seem at odds with maintaining canopy closure to reduce montane mortality, silvicultural prescriptions including group selection and variable retention allow for a diversity of canopy closures across the landscape (*California Forest Practice Rules*, 2022)

It is also unknown if the current regeneration will respond to releases and effectively perpetuate forests. Seedlings and saplings that grow in suppressed conditions are adapted to closed canopies, having shade-foliage with lower photosynthetic capacity than open-grown foliage (Ruel et al., 2000). If given the opportunity to release, these trees must deal with increased light and evaporative demands plus the potential for frost damage (Tesch and Korpela, 1993). As such, canopy openings can fail to elicit substantial increases in growth and lead to understory mortality (Ruel et al., 2000). Red fir saplings across a broad range of sizes (1.5-3.6 m height) and ages (10 -97 years) can release after understory thinning, with younger trees releasing better than older trees (Oliver, 1985). Likewise, grand firs older than 30 years (Ferguson and Adams, 1980) and

white firs older than 45 years do not respond to release as well as younger conspecifics (Helms and Standiford, 1985). Further studies should explore regeneration responses to management, especially in a diverse region such as the Klamath Mountains, as release can be very species-dependent (Ruel et al., 2000).

In conclusion, as California enters another record-setting drought, the importance of fostering resistant and resilient landscapes is highlighted. High mortality rates were found in small trees, montane white pines, and warm, exposed (e.g., ridgetop) coastal environments. Across all study plots, regeneration was old and consisted of few shade-intolerant species. We recommend that disturbances such as fire and thinning be used to promote forest diversity, resistance, resilience, and perpetuation. As possible, these types of disturbance treatments should retain medium-large trees, as these size classes seem to be the least vulnerable to mortality. Where appropriate, artificial regeneration in wildfire footprints or mechanical openings should promote white pines, as these species may fail to persist in northern California due to the demographic trends found in this study. Finally, our work indicates that management efforts should prioritize warm coastal sites and wet montane sites containing white pine, as mortality was greatest in these areas. In closing, we note that the study sites generally represented dense, mixed-conifer stands in northern California and that care should therefore be used if trying to extrapolate these findings to other stand types.

LITERATURE CITED

Adams, H., Zeppel, M., Anderegg, W., Hartmann, H., Landhäusser, S., Tissue, D., Huxman, T., Hudson, P., Franz, T., Allen, C., Anderegg, L., Barron-Gafford, G., Beerling, D., Breshears, D., Brodribb, T., Bugmann, H., Cobb, R., Collins, A., Dickman, L.T., McDowell, N., 2017. A multi-species synthesis of physiological mechanisms in drought-induced tree mortality. Nat. Ecol. Evol. 1, 1285–1291. https://doi.org/10.1038/s41559-017-0248-x

Adams, H.D., Luce, C.H., Breshears, D.D., Allen, C.D., Weiler, M., Hale, V.C., Smith, A.M.S., Huxman, T.E., 2012. Ecohydrological consequences of drought- and infestation- triggered tree die-off: insights and hypotheses. Ecohydrology 5, 145–159. https://doi.org/10.1002/eco.233

Allen, C.D., Macalady, A.K., Chenchouni, H., Bachelet, D., McDowell, N., Vennetier, M., Kitzberger, T., Rigling, A., Breshears, D.D., Hogg, E.H. (Ted), Gonzalez, P., Fensham, R., Zhang, Z., Castro, J., Demidova, N., Lim, J.-H., Allard, G., Running, S.W., Semerci, A., Cobb, N., 2010. A global overview of drought and heat-induced tree mortality reveals emerging climate change risks for forests. For. Ecol. Manag., Adaptation of Forests and Forest Management to Changing Climate 259, 660–684. https://doi.org/10.1016/j.foreco.2009.09.001

Anderegg, W.R.L., Kane, J.M., Anderegg, L.D.L., 2013. Consequences of widespread tree mortality triggered by drought and temperature stress. Nat. Clim. Change 3, 30–36. https://doi.org/10.1038/nclimate1635

Anderegg, W.R.L., Schwalm, C., Biondi, F., Camarero, J.J., Koch, G., Litvak, M., Ogle, K., Shaw, J.D., Shevliakova, E., Williams, A.P., Wolf, A., Ziaco, E., Pacala, S., 2015. Pervasive drought legacies in forest ecosystems and their implications for carbon cycle models. Sci. 349624 528-532 349, 528–532.

Asner, G.P., Brodrick, P.G., Anderson, C.B., Vaughn, N., Knapp, D.E., Martin, R.E., 2016. Progressive forest canopy water loss during the 2012–2015 California drought. Proc. Natl. Acad. Sci. 113, E249–E255. https://doi.org/10.1073/pnas.1523397113

Batllori, E., Lloret, F., Aakala, T., Anderegg, W.R.L., Aynekulu, E., Bendixsen, D.P., Bentouati, A., Bigler, C., Burk, C.J., Camarero, J.J., Colangelo, M., Coop, J.D., Fensham, R., Floyd, M.L., Galiano, L., Ganey, J.L., Gonzalez, P., Jacobsen, A.L., Kane, J.M., Kitzberger, T., Linares, J.C., Marchetti, S.B., Matusick, G., Michaelian, M., Navarro-Cerrillo, R.M., Pratt, R.B., Redmond, M.D., Rigling, A., Ripullone, F., Sangüesa-Barreda, G., Sasal, Y., Saura-Mas, S., Suarez, M.L., Veblen, T.T., Vilà-Cabrera, A., Vincke, C., Zeeman, B., 2020. Forest and woodland replacement patterns following drought-related mortality. Proc. Natl. Acad. Sci. 117, 29720–29729. https://doi.org/10.1073/pnas.2002314117

Beckage, B., Osborne, B., Gavin, D.G., Pucko, C., Siccama, T., Perkins, T., 2008. A rapid upward shift of a forest ecotone during 40 years of warming in the Green Mountains of Vermont. Proc. Natl. Acad. Sci. 105, 4197–4202. https://doi.org/10.1073/pnas.0708921105

Blackburn, R.C., Barber, N.A., Anna, K.F., Buscaglia, R., Jones, H.P., 2021. Monitoring ecological characteristics of a tallgrass prairie using an unmanned aerial vehicle. Restor. Ecol. 29 Suppl S1, e13339-. https://doi.org/10.1111/rec.13339

Bond, B., Meinzer, F., J. Renee, B., 2008. How Trees Influence the Hydrological Cycle in Forest Ecosystems, in: Wood, P., Hannah, D., Sadler, J. (Eds.), Hydroecology and Ecohydrology: Past, Present and Future. Wiley, pp. 7–35.

Bost, D.S., Reilly, M.J., Jules, E.S., DeSiervo, M.H., Yang, Z., Butz, R.J., 2019. Assessing spatial and temporal patterns of canopy decline across a diverse montane landscape in the Klamath Mountains, CA, USA using a 30-year Landsat time series. Landsc. Ecol. 34 2599-2614 34, 2599–2614. https://doi.org/10.1007/s10980-019-00907-7

Breshears, D.D., Cobb, N.S., Rich, P.M., Price, K.P., Allen, C.D., Balice, R.G., Romme, W.H., Kastens, J.H., Floyd, M.L., Belnap, J., Anderson, J.J., Myers, O.B., Meyer, C.W., 2005. Regional Vegetation Die-off in Response to Global-Change-Type Drought. Proc. Natl. Acad. Sci. U. S. A. 102, 15144–15148.

Bunn, A., Korpela, F., Biondi, F., Campelo, F., Mérian, P., Qeadan, F., Zang, C., 2016. dplR: Dendrochronology Program Library in R.

Burns, R.M., Honkala, B.H., 1990. Silvics of North America, Vol. 1: Conifers., U.S.D.A. Forest Service Agriculture Handbook 654. Washington DC.

Byer, S., Jin, Y., 2017. Detecting drought-induced tree mortality in Sierra Nevada forests with time series of satellite data. Remote Sens. 9, 929. https://doi.org/10.3390/rs9090929

California Forest Pest Council, 2020. California Forest Pest Conditions 2020 36.

California Forest Pest Council, 2016. California Forest Pest Conditions 2016. USDA.

California Forest Practice Rules, 2022. , Title 14, California Code of Regulations, Chapters 4, 4.5, and 10.

Clark, J.S., Bell, D.M., Kwit, M.C., Zhu, K., 2014. Competition-interaction landscapes for the joint response of forests to climate change. Glob. Change Biol. 20, 1979–1991. https://doi.org/10.1111/gcb.12425

Clark, J.S., Iverson, L., Woodall, C.W., Allen, C.D., Bell, D.M., Bragg, D.C., D'Amato, A.W., Davis, F.W., Hersh, M.H., Ibanez, I., Jackson, S.T., Matthews, S., Pederson, N., Peters, M., Schwartz, M.W., Waring, K.M., Zimmermann, N.E., 2016. The impacts of increasing drought on forest dynamics, structure, and biodiversity in the United States. Glob. Change Biol. 22, 2329–2352. https://doi.org/10.1111/gcb.13160

Collins, B.M., Bernal, A., York, R.A., Stevens, J.T., Juska, A., Stephens, S.L., 2021. Mixed-conifer forest reference conditions for privately owned timberland in the southern Cascade Range. Ecol. Appl. 31, e02400. https://doi.org/10.1002/eap.2400

Curtis, R.O., Marshall, D.D., 2000. Technical Note: Why Quadratic Mean Diameter? West. J. Appl. For. 15, 137–139. https://doi.org/10.1093/wjaf/15.3.137
Das, A., Battles, J., Stephenson, N.L., van Mantgem, P.J., 2011. The contribution of competition to tree mortality in old-growth coniferous forests. For. Ecol. Manag. 261, 1203–1213. https://doi.org/10.1016/j.foreco.2010.12.035
Das, A.J., Stephenson, N.L., Davis, K.P., 2016. Why do trees die? Characterizing the drivers of background tree mortality. Ecology 97, 2616–2627.
Das, A.J., Stephenson, N.L., Flint, A., Das, T., Mantgem, P.J. van, 2013. Climatic correlates of tree mortality in water- and energy-limited forests. PLOS ONE 8, e69917. https://doi.org/10.1371/journal.pone.0069917
DeCourten, F., 2009. Custom Enrichment Module; Geology of Northern California, 1st edition. ed. Brooks Cole.
DeSiervo, M.H., Jules, E.S., Bost, D.S., De Stigter, E.L., Butz, R.J., 2018. Patterns and drivers of recent tree mortality in diverse conifer forests of the Klamath Mountains, California. For. Sci. 64, 371–382. https://doi.org/10.1093/forsci/fxx022
Diffenbaugh, N.S., Swain, D.L., Touma, D., 2015. Anthropogenic warming has increased drought risk in California. Proc. Natl. Acad. Sci. 112, 3931–3936. https://doi.org/10.1073/pnas.1422385112
Dong, C., MacDonald, G.M., Willis, K., Gillespie, T.W., Okin, G.S., Williams, A.P., 2019. Vegetation Responses to 2012–2016 Drought in Northern and Southern California. Geophys. Res. Lett. 46, 3810–3821. https://doi.org/10.1029/2019GL082137
Dudney, J.C., Nesmith, J.C.B., Cahill, M.C., Cribbs, J.E., Duriscoe, D.M., Das, A.J., Stephenson, N.L., Battles, J.J., 2020. Compounding effects of white pine blister rust, mountain pine beetle, and fire threaten four white pine species. Ecosphere 11. https://doi.org/10.1002/ecs2.3263
Emery, N.C., D'Antonio, C.M., Still, C.J., 2018. Fog and live fuel moisture in coastal California shrublands. Ecosphere 9, e02167. https://doi.org/10.1002/ecs2.2167
Entekhabi, D., Njoku, E.G., O'Neill, P.E., Kellogg, K.H., Crow, W.T., Edelstein, W.N., Entin, J.K., Goodman, S.D., Jackson, T.J., Kimball, J., Piepmeier, J.R., Koster, R.D., Martin, N., McDonald, K.C., Moghaddam, E.J., 2022. spatialEco. R package version 1.3-3.
Erdle, T., n.d. Measurement of Tree Basal Area and Volume.
Ferguson, D.E., Adams, D.L., 1980. Response of advance grand fir regeneration to overstory removal in Northern Idaho. For. Sci. 26, 537–545. https://doi.org/10.1093/forestscience/26.4.537
Fettig, C.J., Klepzig, K.D., Billings, R. f, Munson, A.S., Nebeker, T.E., Negron, J.F., Nowak, J.T., 2007. The effectiveness of vegetation management practices for prevention and control of bark beetle infestations in coniferous forests of the western and southern United States. For. Ecol. Manag. 2381-3 24-53.

Fettig, C.J., Mortenson, L.A., Bulaon, B.M., Foulk, P.B., 2019. Tree mortality following drought in the central and southern Sierra Nevada, California, U.S. For. Ecol. Manag. 432, 164–178. https://doi.org/10.1016/j.foreco.2018.09.006
Field, C., Merino, J., Mooney, H.A., 1983. Compromises between water-use efficiency and nitrogen-use efficiency in five species of California evergreens. Oecologia 60, 384–389. https://doi.org/10.1007/BF00376856
Fogel, R., Cromack, K., Biome, U.S.I.B.P.C.F., Washington, U. of, 1973. Terrestrial decomposition: a synopsis [WWW Document].
Fowells, H.A., 1965. Natural Regeneration in Relation to Environment in the Mixed Conifer Forest Type of California. Pacific Southwest Forest and Range Experiment Station, Forest Service, U.S. Department of Agriculture.
Friedman, J., Hastie, T., Tibshirani, R., 2010. Regularization paths for generalized linear models via coordinate descent. J. Stat. Softw. 33, 1–22.
Fryer, J.L., 2008. Notholithocarpus densiflorus [WWW Document]. Fire Eff. Inf. Syst. URL https://www.fs.fed.us/database/feis/plants/tree/notden/all.html#30 (accessed 3.15.22).
Furniss, R.L., 1977. Western Forest Insects. Department of Agriculture, Forest Service.
Goodwin, M.J., Zald, H.S.J., North, M.P., Hurteau, M.D., 2021. Climate-driven tree mortality and fuel aridity increase wildfire's potential heat flux. Geophys. Res. Lett. 48, e2021GL094954. https://doi.org/10.1029/2021GL094954
Goulden, M.L., Bales, R.C., 2019. California forest die-off linked to multi-year deep soil drying in 2012-2015 drought. Nat. Geosci. 12, 632-+. https://doi.org/10.1038/s41561-019-0388-5
Grantham, T., 2018. North Coast Region Report (California's Fourth Climate Change Assessment).
Griffin, D., Anchukaitis, K.J., 2014. How unusual is the 2012–2014 California drought? Geophys. Res. Lett. 41, 9017–9023. https://doi.org/10.1002/2014GL062433
Griffin, J.R., Critchfield, W.B., 1972. The distribution of forest trees in California. Res Pap. PSW-RP-82 Berkeley CA Pac. Southwest For. Range Exp. Stn. For. Serv. US Dep. Agric. 60 P 082.
Griffith, R.S., 1992. Pinus monticola (U.S. Department of Agriculture, Forest Service, Rocky Mountain Research Station, Fire Sciences Laboratory).
Harmon, M.E., Woodall, C.W., Fasth, B., Sexton, J., Yatkov, Misha., 2011. Differences between standing and downed dead tree wood density reduction factors: A comparison across decay classes and tree species (No. NRS-RP-15). U.S. Department of Agriculture, Forest Service, Northern Research Station, Newtown Square, PA. https://doi.org/10.2737/NRS-RP-15
Hartmann, H., 2015. Carbon starvation during drought-induced tree mortality – are we chasing a myth? J. Plant Hydraul. 2, e005.
Heinze, G., Wallisch, C., Dunkler, D., 2018. Variable selection - A review and recommendations for the practicing statistician. Biom. J. Biom. Z. 60, 431–449. https://doi.org/10.1002/bimj.201700067

Helms, J.A., Standiford, R.B., 1985. Predicting release of advance reproduction of mixed conifer species in California following overstory removal. For. Sci. 31, 3–15. https://doi.org/10.1093/forestscience/31.1.3
Holmes, R.L., 1984. Computer-assisted quality control in tree-ring dating and measurement. Tree-Ring Bull. 43, 51–67.
Hughes, M.K., Brown, P.M., 1992. Drought frequency in central California since 101 B.C. recorded in giant sequoia tree rings. Clim. Dyn. 6, 161–167. https://doi.org/10.1007/BF00193528
James, G., Witten, D., Hastie, T., Tibshirani, R., 2021. An Introduction to Statistical Learning: with Applications in R. Springer Nature.
Johnstone, J.A., Dawson, T.E., 2010. Climatic context and ecological implications of summer fog decline in the coast redwood region. Proc. Natl. Acad. Sci. 107, 4533–4538. https://doi.org/10.1073/pnas.0915062107
Jones, M., Lee, C., Valachovic, Y., 2019. Balsam Wooly Adelgid in California.
Jules, E.S., Carroll, A.L., Garcia, A.M., Steenbock, C.M., Kauffman, M.J., 2014. Host heterogeneity influences the impact of a non-native disease invasion on populations of a foundation tree species. Ecosphere 5, art105. https://doi.org/10.1890/ES14-00043.1
Kauffmann, M., 2012. Conifer Country: a natural history and hiking guide to 35 conifers of the Klamath Mountain region. Back Country Press.
Kayes, L.J., Tinker, D.B., 2012. Forest structure and regeneration following a mountain pine beetle epidemic in southeastern Wyoming. For. Ecol. Manag. 263, 57–66. https://doi.org/10.1016/j.foreco.2011.09.035
Keyes, C., Manso, R., 2015. Climate-influenced ponderosa pine (Pinus ponderosa) seed masting trends in western Montana, USA. For. Syst. 24. https://doi.org/10.5424/fs/2015241-05606
Kimmey, J.W., Wagener, W.W., 1961. Spread of White Pine Blister Rust from Ribes to Sugar Pine in California and Oregon. U.S. Department of Agriculture.
Kitzberger, T., Steinaker, D.F., Veblen, T.T., 2000. Effects of climatic variability on facilitation of tree establishment in Northern Patagonia. Ecology 81, 1914–1924. https://doi.org/10.1890/0012-9658(2000)081[1914:EOCVOF]2.0.CO;2
Knight, C.A., Anderson, L., Bunting, M.J., Champagne, M., Clayburn, R.M., Crawford, J.N., Klimaszewski-Patterson, A., Knapp, E.E., Lake, F.K., Mensing, S.A., Wahl, D., Wanket, J., Watts-Tobin, A., Potts, M.D., Battles, J.J., 2022. Land management explains major trends in forest structure and composition over the last millennium in California's Klamath Mountains. Proc. Natl. Acad. Sci. 119, e2116264119. https://doi.org/10.1073/pnas.2116264119
Knudsen, D.C., 1992. Generalizing poisson regression: including apriori information using the method of offsets. Prof. Geogr. 44, 202–208. https://doi.org/10.1111/j.0033-0124.1992.00202.x
Lauder, J.D., Moran, E.V., Hart, S.C., 2019. Fight or flight? Potential tradeoffs between drought defense and reproduction in conifers. Tree Physiol. 39, 1071–1085. https://doi.org/10.1093/treephys/tpz031

Logan, J.A., Régnière, J., Powell, J.A., 2003. Assessing the impacts of global warming on forest pest dynamics. Front. Ecol. Environ. 1, 130–137. https://doi.org/10.1890/1540-9295(2003)001[0130:ATIOGW]2.0.CO;2
Manion, P.D., 1981. Tree Disease Concepts. Prentice-Hall.
Mariani, M., Fletcher, M.-S., Holz, A., Nyman, P., 2016. ENSO controls interannual fire activity in southeast Australia. Geophys. Res. Lett. 43, 10,891-10,900. https://doi.org/10.1002/2016GL070572
Martínez-Vilalta, J., Sala, A., Piñol, J., 2004. The hydraulic architecture of Pinaceae – a review. Plant Ecol. 171, 3–13. https://doi.org/10.1023/B:VEGE.0000029378.87169.b1
McDowell, N., Pockman, W.T., Allen, C.D., Breshears, D.D., Cobb, N., Kolb, T., Plaut, J., Sperry, J., West, A., Williams, D.G., Yepez, E.A., 2008. Mechanisms of plant survival and mortality during drought: why do some plants survive while others succumb to drought? New Phytol. 178, 719–739. https://doi.org/10.1111/j.1469-8137.2008.02436.x
McDowell, N.G., 2011. Mechanisms linking drought, hydraulics, carbon metabolism, and vegetation mortality. Plant Physiol. 155, 1051–1059. https://doi.org/10.1104/pp.110.170704
Meehl, G.A., Tebaldi, C., 2004. More intense, more frequent, and longer lasting heat waves in the 21st century. Science 305, 994–997. https://doi.org/10.1126/science.1098704
Millar, C.I., Stephenson, N.L., 2015. Temperate forest health in an era of emerging megadisturbance. Science 349, 823–826. https://doi.org/10.1126/science.aaa9933
Miller, A.E., Wilson, T.L., Sherriff, R.L., Walton, J., 2017. Warming drives a front of white spruce establishment near western treeline, Alaska. Glob. Change Biol. 23, 5509–5522. https://doi.org/10.1111/gcb.13814
Minore, D., 1986. Germination, survival and early growth of conifer seedlings in two habitat types. For. Serv. United State Dep. Agric. 63.
National Biological Information Infrastructure, (NBII), Invasive Species Specialist, (ISSG), 2005. Ecology of Cronartium ribicola (Global Invasive Species Database).
Norazan, M.R., Midi, H., Imon, A.H.M.R., 2009. Estimating regression coefficients using weighted bootstrap with probability. WSEAS Trans. Math. 8, 362–371.
Northern California Indian Development Council, 2021.
O'Hara, K.L., Leonard, L.P., Keyes, C.R., 2012. Variable-density thinning and a marking paradox: comparing prescription protocols to attain stand variability in coast redwood. West. J. Appl. For. 27, 143–149. https://doi.org/10.5849/wjaf.11-042
Oliver, C.D., Larson, B.A., 1996. Forest Stand Dynamics, Update Edition. EliScholar 222,224.
Oliver, W.W., 1985. Growth of California red fir advance regeneration after overstory removal and thinning. Res Pap. PSW-RP-180 Berkeley CA US Dep. Agric. For. Serv. Pac. Southwest For. Range Exp. Stn. 12 P 180. https://doi.org/10.2737/PSW-RP-180

Orwig, D.A., Abrams, M.D., 1997. Variation in radial growth responses to drought among species, site, and canopy strata. Trees 11, 474–484. https://doi.org/10.1007/s004680050110
Paradis, E., 2022. Moran's Autocorrelation Coefficient in Comparative Methods 8.
Pirtel, N.L., Hubbard, R.M., Bradford, J.B., Kolb, T.E., Litvak, M.E., Abella, S.R., Porter, S.L., Petrie, M.D., 2021. The aboveground and belowground growth characteristics of juvenile conifers in the southwestern United States. Ecosphere 12, e03839. https://doi.org/10.1002/ecs2.3839
Redmond, M.D., Barger, N.N., 2013. Tree regeneration following drought- and insect-induced mortality in piñon–juniper woodlands. New Phytol. 200, 402–412. https://doi.org/10.1111/nph.12366
Robinson, W., 2021. Influences on conifer drought responses in northern California. Cal Poly Humboldt Thesis Proj.
Rodman, K.C., Veblen, T.T., Battaglia, M.A., Chambers, M.E., Fornwalt, P.J., Holden, Z.A., Kolb, T.E., Ouzts, J.R., Rother, M.T., 2020. A changing climate is snuffing out post-fire recovery in montane forests. Glob. Ecol. Biogeogr. n/a. https://doi.org/10.1111/geb.13174
Roletti, G., in press. Effects of Competition, Climate, and Site and Tree Characteristics on Growth. Cal Poly Humboldt Thesis Proj.
Ruel, J.-C., Messier, C., Claveau, Y., Doucet, R., Comeau, P., 2000. Morphological indicators of growth response of coniferous advance regeneration to overstorey removal in the boreal forest. For. Chron. 76, 633–642. https://doi.org/10.5558/tfc76633-4
Schriver, M., Sherriff, R.L., Varner, J.M., Quinn-Davidson, L., Valachovic, Y., 2018. Age and stand structure of oak woodlands along a gradient of conifer encroachment in northwestern California. Ecosphere 9, e02446. https://doi.org/10.1002/ecs2.2446
Schwandt, J., Kearns, H., Byler, J., 2013. White pine blister rust general ecology and managment. Insect Dis. Manag. Ser. 14.2.
Sevanto, S., 2014. Phloem transport and drought. J. Exp. Bot. 65, 1751–1759.
Sherriff, R.L., Kauffman, M., Garwood, J., in press. Klamath climate chapter. Back Country Press.
Skinner, C.N., Taylor, A.H., 2006. Southern Cascades Bioregion, in: Fire in California's Ecosystems. University of California Press. https://doi.org/10.1525/california/9780520246058.003.0010
Skinner, C.N., Taylor, A.H., Agee, J.K., 2006. Klamath Mountains Bioregion, in: Sugihara, N. (Ed.), Fire in California's Ecosystems. University of California Press, pp. 170–194. https://doi.org/10.1525/california/9780520246058.003.0009
Smith, D.M., Larson, D., Kelty, M., Ashton, P.M.S., 1996. The Response of Individual Trees to Thinning and Pruning, in: The Practice of Silviculture: Applied Forest Ecology. Wiley, pp. 47–68.

Soland, K., Kerhoulas, L., Kerhoulas, N., Teraoka, J.R., 2021. Second-growth redwood forest responses to restoration treatments. For. Ecol. Manag. 496, 119370. https://doi.org/10.1016/j.foreco.2021.119370

Soong, J.L., Janssens, I.A., Grau, O., Margalef, O., Stahl, C., Van Langenhove, L., Urbina, I., Chave, J., Dourdain, A., Ferry, B., Freycon, V., Herault, B., Sardans, J., Peñuelas, J., Verbruggen, E., 2020. Soil properties explain tree growth and mortality, but not biomass, across phosphorus-depleted tropical forests. Sci. Rep. 10, 2302. https://doi.org/10.1038/s41598-020-58913-8

Speer, J., 2010. Fundamentals of Tree Ring Research.

Steel, Z., Goodwin, M., Meyer, M., Fricker, G.A., Zald, H., Hurteau, M., North, M.P., 2021. Do forest fuel reduction treatments confer resistance to beetle infestation and drought mortality? Ecosphere. https://doi.org/10.32942/osf.io/bwmg2

Stephens, S.L., Collins, B.M., Fettig, C.J., Finney, M.A., Hoffman, C.M., Knapp, E.E., North, M.P., Safford, H., Wayman, R.B., 2018. Drought, tree mortality, and wildfire in forests adapted to frequent fire. BioScience 68, 77–88. https://doi.org/10.1093/biosci/bix146

Stephens, S.L., Westerling, A.L., Hurteau, M.D., Peery, M.Z., Schultz, C.A., Thompson, S., 2020. Fire and climate change: conserving seasonally dry forests is still possible. Front. Ecol. Environ. 18, 354–360. https://doi.org/10.1002/fee.2218

Stephenson, N., 1998. Actual evapotranspiration and deficit: biologically meaningful correlates of vegetation distribution across spatial scales. J. Biogeogr. 25, 855–870. https://doi.org/10.1046/j.1365-2699.1998.00233.x

Stephenson, N.L., 1990. Climatic control of vegetation distribution: the role of the water balance. Am. Nat. 135, 649–670. https://doi.org/10.1086/285067

Stephenson, N.L., Das, A.J., Ampersee, N.J., Bulaon, B.M., Yee, J.L., 2019. Which trees die during drought? The key role of insect host-tree selection. J. Ecol. 107, 2383–2401. https://doi.org/10.1111/1365-2745.13176

Sthultz, C.M., Gehring, C.A., Whitham, T.G., 2007. Shifts from competition to facilitation between a foundation tree and a pioneer shrub across spatial and temporal scales in a semiarid woodland. New Phytol. 173, 135–145. https://doi.org/10.1111/j.1469-8137.2006.01915.x

Stubblefield, A.P., Reddy, K., 2021. Measurement and prediction of water consumption by Douglas-fir, Northern California, USA. Ecohydrology 15, e2388. https://doi.org/10.1002/eco.2388

Taylor, A.H., Skinner, C.N., 1998. Fire history and landscape dynamics in a late-successional reserve, Klamath Mountains, California, USA. For. Ecol. Manag. 111, 285–301. https://doi.org/10.1016/S0378-1127(98)00342-9

Telewski, F.W., 1993. Determining the germination date of woody plants: a proposed method for locating the root/shoot Interface.

Tesch, S.D., Korpela, E.J., 1993. Douglas-fir and white fir advance regeneration for renewal of mixed-conifer forests. Can. J. For. Res. 23, 1427–1437. https://doi.org/10.1139/x93-180

U.S. Drought Monitor, 2022. Current U.S. Drought Monitor Conditions for California [WWW Document]. Drought.gov. URL https://www.drought.gov/states/california (accessed 3.7.22).
USDA, 2021. Aerial Detection Survey: 2021 Summary Report (US Forest Service, Davis, CA).
USDA, 2020. 2019 aerial survey results: California (US Forest Service, Davis, CA).
USDA, n.d. Web Soil Survey - Home [WWW Document]. URL https://websoilsurvey.sc.egov.usda.gov/App/HomePage.htm (accessed 5.2.22).
Ustin, S.L., Roberts, D.A., Gamon, J.A., Asner, G.P., Green, R.O., 2004. Using imaging spectroscopy to study ecosystem processes and properties. BioScience 54, 523. https://doi.org/10.1641/0006-3568(2004)054[0523:UISTSE]2.0.CO;2
van Mantgem, P.J., Caprio, A.C., Stephenson, N.L., Das, A.J., 2016. Does prescribed fire promote resistance to drought in low elevation forests of the Sierra Nevada, California, USA? Fire Ecol. 12, 13–25. https://doi.org/10.4996/fireecology.1201013
van Mantgem, P.J., Stephenson, N.L., Keeley, J.E., 2006. Forest reproduction along a climatic gradient in the Sierra Nevada, California. For. Ecol. Manag. 225, 391–399. https://doi.org/10.1016/j.foreco.2006.01.015
Vernon, M.J., Sherriff, R.L., van Mantgem, P., Kane, J.M., 2018. Thinning, tree-growth, and resistance to multi-year drought in a mixed-conifer forest of northern California. For. Ecol. Manag. 422, 190–198. https://doi.org/10.1016/j.foreco.2018.03.043
Western Regional Climate Center, n.d. Callahan, California - Climate Summary [WWW Document]. URL https://wrcc.dri.edu/cgi-bin/cliMAIN.pl?ca1316 (accessed 4.28.22).
Whittaker, R.H., 1961. Vegetation history of the Pacific coast states and the “central” significance of the Klamath region. Madroño 16, 5–23.
Whittaker, R.H., 1960. Vegetation of the Siskiyou Mountains, Oregon and California. Ecol. Monogr. 30, 279–338. https://doi.org/10.2307/1943563
Williams, A.P., Seager, R., Abatzoglou, J.T., Cook, B.I., Smerdon, J.E., Cook, E.R., 2015. Contribution of anthropogenic warming to California drought during 2012–2014. Geophys. Res. Lett. 42, 6819–6828. https://doi.org/10.1002/2015GL064924
Wilson, A.M., Jetz, W., n.d. Global 1-km Cloud Cover [WWW Document]. URL https://earthenv-dot-map-of-life.appspot.com/3/0.000/0.000?collections=cloud&layers=Seasonality (accessed 3.11.22).
Wood, D.L., Koerber, T.W., Scharpf, R.F., Storer, A.J., 2003. Pests of the Native California Conifers, 1st ed. University of California Press.
Wright, M., Sherriff, R.L., Miller, A.E., Wilson, T., 2018. Stand basal area and temperature interact to influence growth in white spruce in southwest Alaska. Ecosphere 9, e02462. https://doi.org/10.1002/ecs2.2462

Young, D.J.N., Meyer, M., Estes, B., Gross, S., Wuenschel, A., Restaino, C., Safford, H.D., 2020. Forest recovery following extreme drought in California, USA: natural patterns and effects of pre-drought management. Ecol. Appl. 30, e02002. https://doi.org/10.1002/eap.2002

Young, D.J.N., Stevens, J.T., Earles, J.M., Moore, J., Ellis, A., Jirka, A.L., Latimer, A.M., 2017. Long-term climate and competition explain forest mortality patterns under extreme drought. Ecol. Lett. 20, 78–86. https://doi.org/10.1111/ele.12711

Zahari, S., Mohamed Ramli, N., Moktar, B., 2014. Bootstrapped parameter estimation in ridge regression with multicollinearity and multiple outliers. J. Appl. Environ. Biol. Sci. 4, 150–156.

Zanne, A.E., Oberle, B., Dunham, K.M., Milo, A.M., Walton, M.L., Young, D.F., Bardgett, R., 2015. A deteriorating state of affairs: How endogenous and exogenous factors determine plant decay rates. J. Ecol. 103, 1421–1431. https://doi.org/10.1111/1365-2745.12474

Zouhar, K., 2001. Abies concolor [WWW Document]. Fire Eff. Inf. Syst. URL https://www.fs.fed.us/database/feis/plants/tree/abicon/all.html (accessed 3.15.22).

APPENDICES

Appendix A

Appendix A. Independent variables used in analyses.

Table A 1. Descriptions of each independent variable used in statistical modeling or graphical summaries of mortality and regeneration trends in northern California.

Covariate	Description	Data Source
Competition		
Canopy Closure (CanClos)	Percent of ground that is under at least one layer of canopy.	Canopy cover was measured in the 0.1 ha subplot using a Densiometer at 5 locations: plot center and 8.9 m in each cardinal direction from plot center. At each location, four measurements were taken, one in each cardinal direction, and averaged.
Trees per Hectare (TPH)	Number of trees present within one hectare.	Total number of live trees were recorded in the 0.1 ha plot and multiplied by ten to extrapolate to 1 ha.
Quadratic Mean Diameter (QMD)	Calculated from individual tree breast height diameter and the total number of trees per ha.	QMD was calculated based on published equations (Curtis and Marshall 2000).
Topography		
Topographic Position Index (TPI)	A measure of elevation at a site relative to surrounding average elevations, with higher TPIs associated with upper slope positions, and negative values with valleys (Weiss 2001).	TPI was calculated for each site using its central coordinates and a 7-cell neighborhood. TPI values were obtained using the *spatialEco* R package (Entekhabi et al., 2022).

Covariate	Description	Data Source
Ground		
Percent Ground Cover	The proportion of ground that is covered by at least one layer of vegetative cover (herbaceous plants and shrubs included).	Percent ground cover was ocularly estimated in the 0.1 ha subplot.
Climate		
Mean Annual Climatic Water Deficit (CWD)	Measure of annual evaporative demand that exceeds available water; used for the superposed epoch analysis.	Monthly values were sourced from the TerraClimat database (http://www.climatologylab.org/gridmet.html) and then averaged for each year.
30-Year Mean Annual Precipitation or Mean Precipitation (PPT_{30})	Mean annual rainfall per location; used to characterize long-term moisture availability at each site.	Monthly values were sourced from the TerraClimat database (http://www.climatologylab.org/gridmet.html) and then averaged to obtain annual values, and then averaged across the 30-year time frame 1990-2020.
30-Year Mean Annual Maximum Temperature or Mean Maximum Temperature ($T_{max,30}$)	Maximum annual temperature; used to characterize sites.	Monthly values were sourced from the TerraClimat database (http://www.climatologylab.org/gridmet.html) and then averaged to obtain annual values, and then averaged across the 30-year time frame 1990-2020.
Tree		
Diameter at Breast Height (DBH)	Characterizes the size of a tree; used to compare mortality patterns among size classes.	DBH was measured in the field using a Spencer's tape at 1.37 m height.
Tree Species	The study included all tree species within the northern California ranges of *Picea breweriana*, *Abies magnifica* var. *shastensis*, *Pinus monticola*, *Picea sitchensis*, *Pinus lambertiana*, *Tsuga heterophylla*.	Species present were recorded for each 0.25 ha plot.

Covariate	Description	Data Source
Shade Tolerance	Regeneration quantities were compared by three categories of shade tolerance (shade-tolerant, moderately shade-tolerant, and shade-intolerant), with hardwoods counted in a separate category.	Species were identified in the field and sorted based on information in the USFS Fire Effects Information System's (https://www.feis-crs.org/feis/) species descriptions.

Appendix B

Appendix B. Decay classes used for classifying dead trees.

Table B 1. Each dead tree within the 0.25 ha plot was categorized into one of the 1 to 5 decay classes. Abbreviations: HW (heartwood) and SW (sapwood). Decay classes based on Fogel et al., 1973 and Harmon et al., 2011.

Decay Class	Criteria
1	All limbs and branches present; top present; all bark remains; SW intact with minimal decay; HW sound and hard.
2	A few limbs but no fine branches; top may be broken; variable bark remaining; SW sloughing with advanced decay; HW sound at base but beginning to decay in outer upper bole.
3	Only limb stubs exist; top broken; variable remaining bark; SW sloughing; HW has advanced decay in upper bole and beginning to decay at bole base.
4	Few or no limb stubs remain; top broken; variable remaining bark; SW sloughing; HW has advanced decay at bole base and sloughing in upper bole.
5	No evidence of branches remains; top broken; < 20% of bark remains; SW gone; HW sloughing throughout.

Appendix C

Appendix C. Dead trees dated by decay class and environment (coastal and montane).

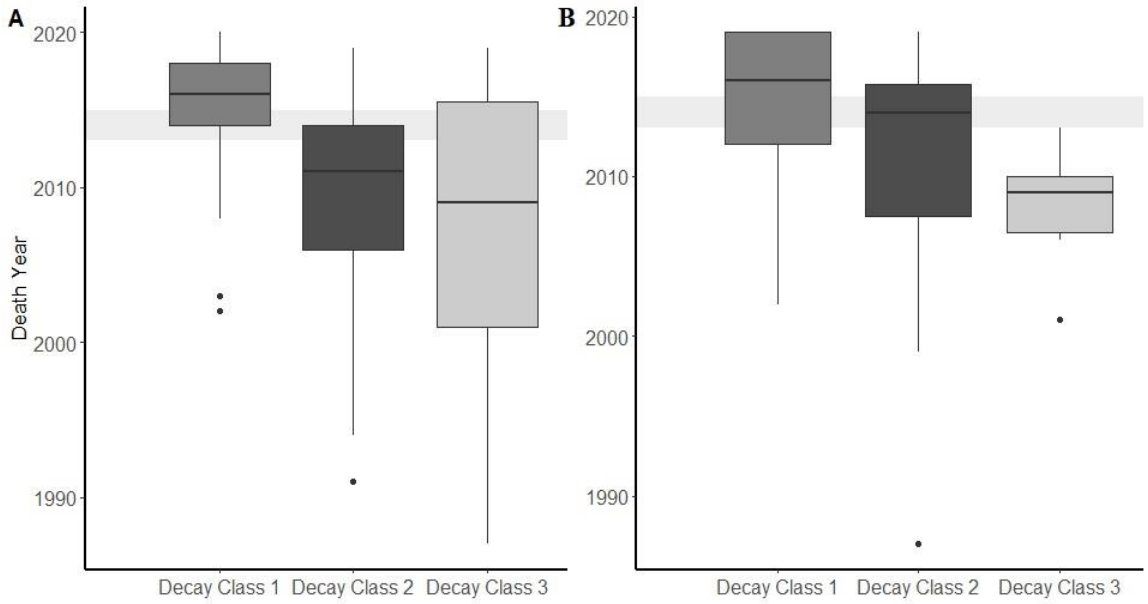

Figure C 1. A) Montane death years by decay class 1 (*n* = 82, median = 2016, mean = 2016), decay class 2 (*n* = 55, median = 2011, mean = 2010), and decay class 3 (*n* = 27, median = 2009, mean = 2008) and B) Coastal death years by decay class 1 (*n* = 14, median = 2014, mean = 2013), decay class 2 (*n* = 22, median = 2008, mean = 2008), and decay class 3 (*n* = 17, median = 2008, mean = 2006).

Appendix D

Appendix D. Difference in root-mean squared errors (RMSEs) distributions for mortality and regeneration ridge regression models.

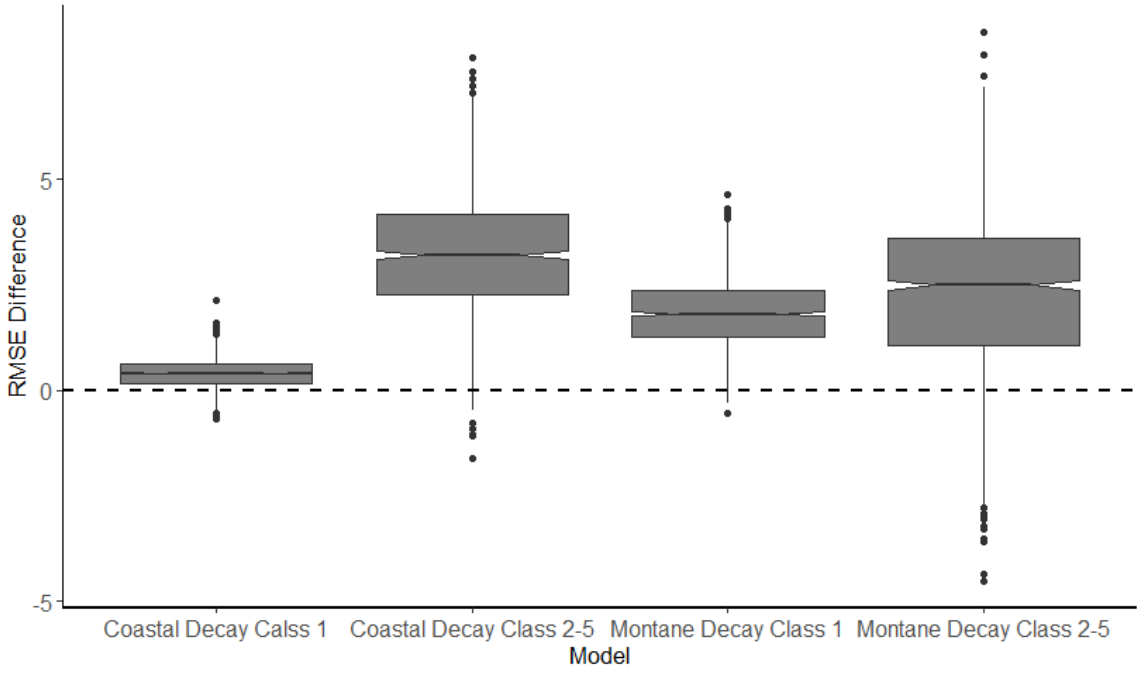

Figure D 1. Difference in root-mean squared errors (RMSEs) between the null and full models measuring rate of coastal decay class 1 trees, coastal decay class 2-5 trees, montane decay class 1 trees, and montane decay class 2-5 trees. Positive values indicate the full model's RMSE was lower than that of the null model's; the difference can range between the response variable's minimum and maximum values.

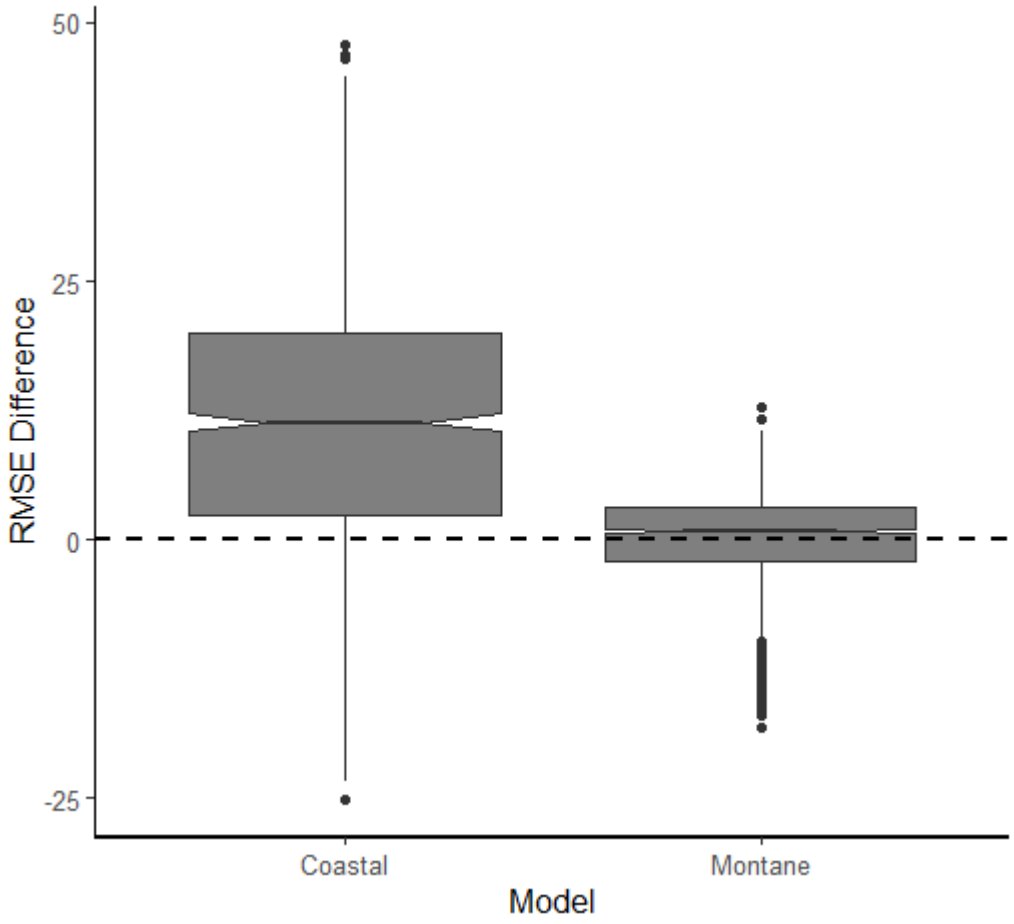

Figure D 2. Difference in root-mean squared errors (RMSEs) between the null and full models for measuring the quantities of coastal and montane regeneration. Positive values indicate the full model's RMSE was lower than that of the null model's; the difference can range between the response variable's minimum and maximum values.

Appendix E

Appendix E. Supplementary ridge regression results for the models predicting total mortality rates (all decay classes) in montane and coastal environments.

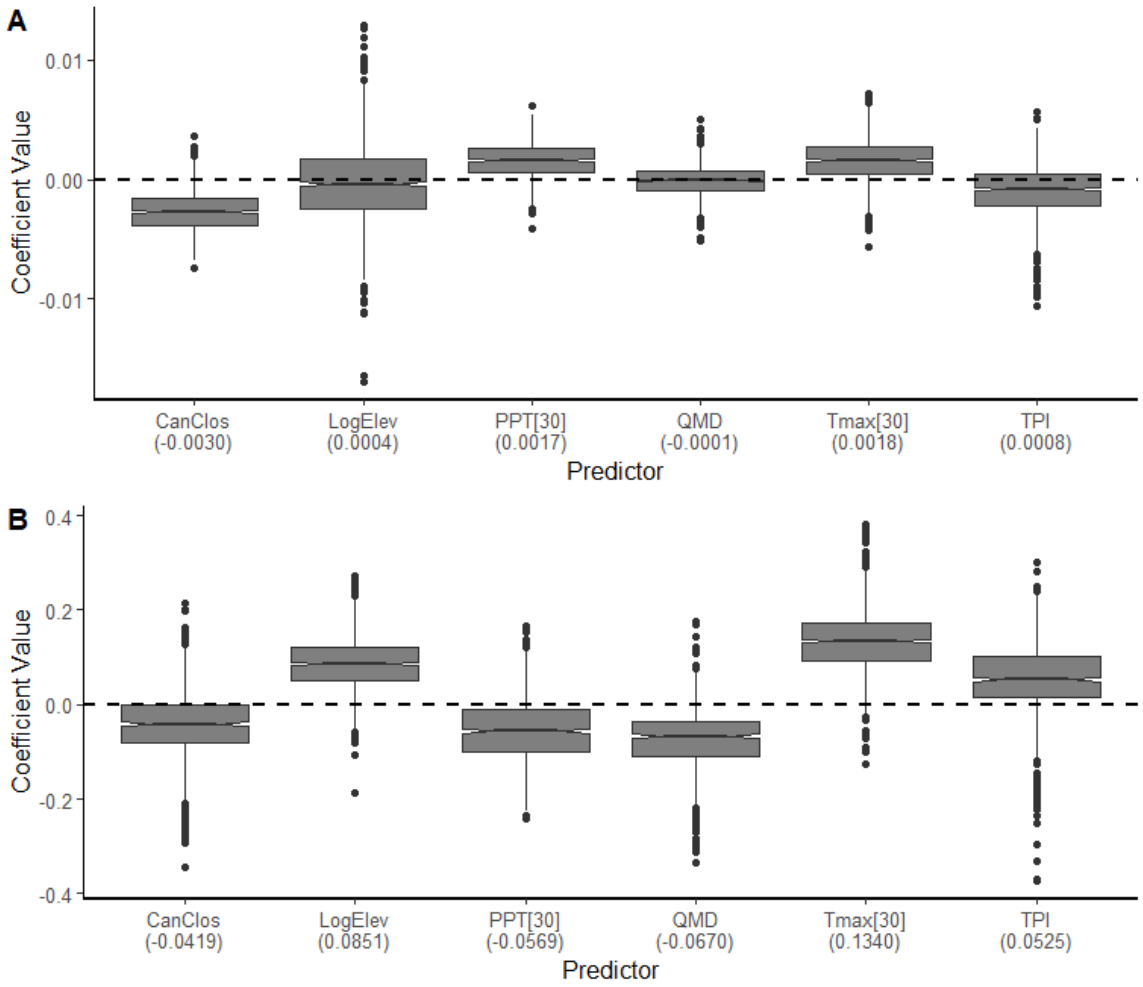

Figure E 1. Covariate coefficient distributions from the bootstrap ridge estimation; intercept coefficient not included due to scale limitation. A) All montane mortality rates; intercept median coefficient was -1.80 with 95% confidence interval ranging from -2.08 to -1.58. B) All coastal mortality rates; intercept median coefficient was -1.70 with 95% confidence interval ranging from -1.85 to -1.56. Abbreviations: CanClos (Canopy Closure), LogElev (log of elevation), PPT[30] (30-year mean annual precipitation), QMD (quadratic mean diameter), TMax[30] (30-year mean annual maximum temperature), and TPI (topographic position index). Parenthetical numbers indicate median coefficient values. Note differing vertical axis scales between panels.

Table E 1. Descriptive statistics for models predicting the rate of all dead trees in montane and coastal environments. RMSE indicates root-mean squared error.

Model	R^2	Response #	Full Model RMSE	RMSE Difference (Null - Full)
Montane	0.21	17.5	17.1	4.2
Coastal	0.72	11.5	6.3	3.6

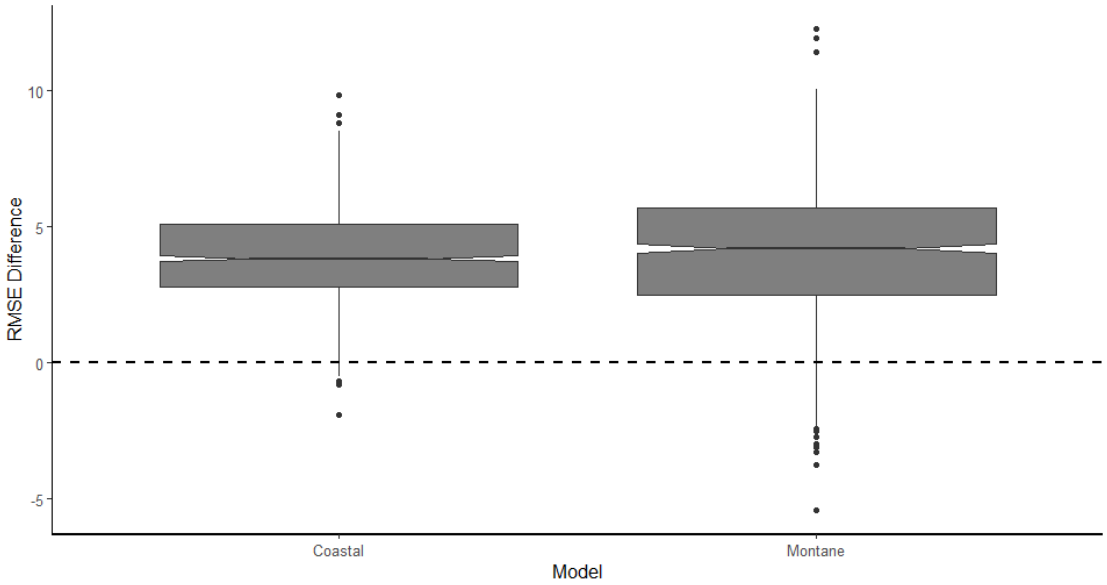

Figure E 2. Difference in root-mean squared errors (RMSEs) between the null and the full models for rate of total mortality in coastal and montane environments. Positive values indicate the full model's RMSE was lower than that of the null model's; the difference can range between the response variable's minimum and maximum values.

Appendix F

Appendix F. Outputs from the superposed epoch analysis (SEA) for montane mortality and regeneration models.

Table F 1. Output table from superposed epoch analysis (SEA) for montane mortality events. Abbreviations include: se (superposed epoch, i.e., the scaled mean climatic water deficit [CWD] for the event years), se.unscaled (the unscaled superposed epoch, i.e., the mean CWD for the event years), and ci (confidence interval).

lag	se	se.unscaled	*p*	ci.95.lower	ci.95.upper	ci.99.lower	ci.99.upper
-4	-0.522	335.185	0.464	-1.161	0.250	-1.374	0.502
-3	-0.289	348.908	0.629	-1.088	0.300	-1.320	0.551
-2	0.005	366.314	0.048	-1.148	0.085	-1.307	0.276
-1	0.370	387.858	0.046	-1.088	0.473	-1.319	0.764
0	0.366	387.651	0.033	-1.088	0.415	-1.278	0.701
1	0.575	399.989	0.025	-0.972	0.563	-1.169	0.795
2	0.732	409.259	0.042	-0.581	0.806	-0.764	0.961
3	0.575	399.985	0.131	-0.239	0.812	-0.347	0.949
4	0.523	396.924	0.451	-0.036	0.995	-0.163	1.180

Table F 2. Output table from superposed epoch analysis (SEA) for montane regeneration events. Abbreviations include: se (superposed epoch, i.e., the scaled mean climatic water deficit [CWD] for the event years), se.unscaled (the unscaled superposed epoch, i.e., the mean CWD for the event years), and ci (confidence interval).

lag	se	se.unscaled	*p*	ci.95.lower	ci.95.upper	ci.99.lower	ci.99.upper
-4	-0.665	294.323	0.077	-0.851	0.544	-1.085	0.704
-3	-0.419	310.836	0.212	-0.854	0.534	1.048	0.672
-2	-0.059	335.023	0.602	-0.768	0.565	-0.983	0.864
-1	-0.746	288.905	0.025	-0.738	0.606	-0.899	0.846
0	0.221	353.830	0.279	-0.619	0.713	-0.840	0.885
1	0.125	347.379	0.446	-0.601	0.749	-0.770	1.013
2	-0.125	330.559	0.271	-0.545	0.789	-0.758	1.041
3	-0.419	310.880	0.052	-0.542	0.772	-0.692	1.115
4	0.301	359.183	0.289	-0.557	0.759	-0.699	0.902

Appendix G

Appendix G. White pine (*Pinus lambertiana* and *Pinus monticola*) mortality rate by mean 30-year (1990-2020) precipitation (PPT_{30}). A single predictor negative binomial mixed effect model with plot as a random effect found a significant positive relationship between PPT_{30} and rate of white pine mortality (coefficient= 0.003, $p = 0.001$, $t = 3.86$, df = 25, $R^2 = 0.41$). Rate of white pine mortality was calculated as the number of dead trees per 0.25 ha plot divided by an offset (the number of live trees in the 0.10 ha plot plus the number of dead white pines in the 0.25 ha plot).

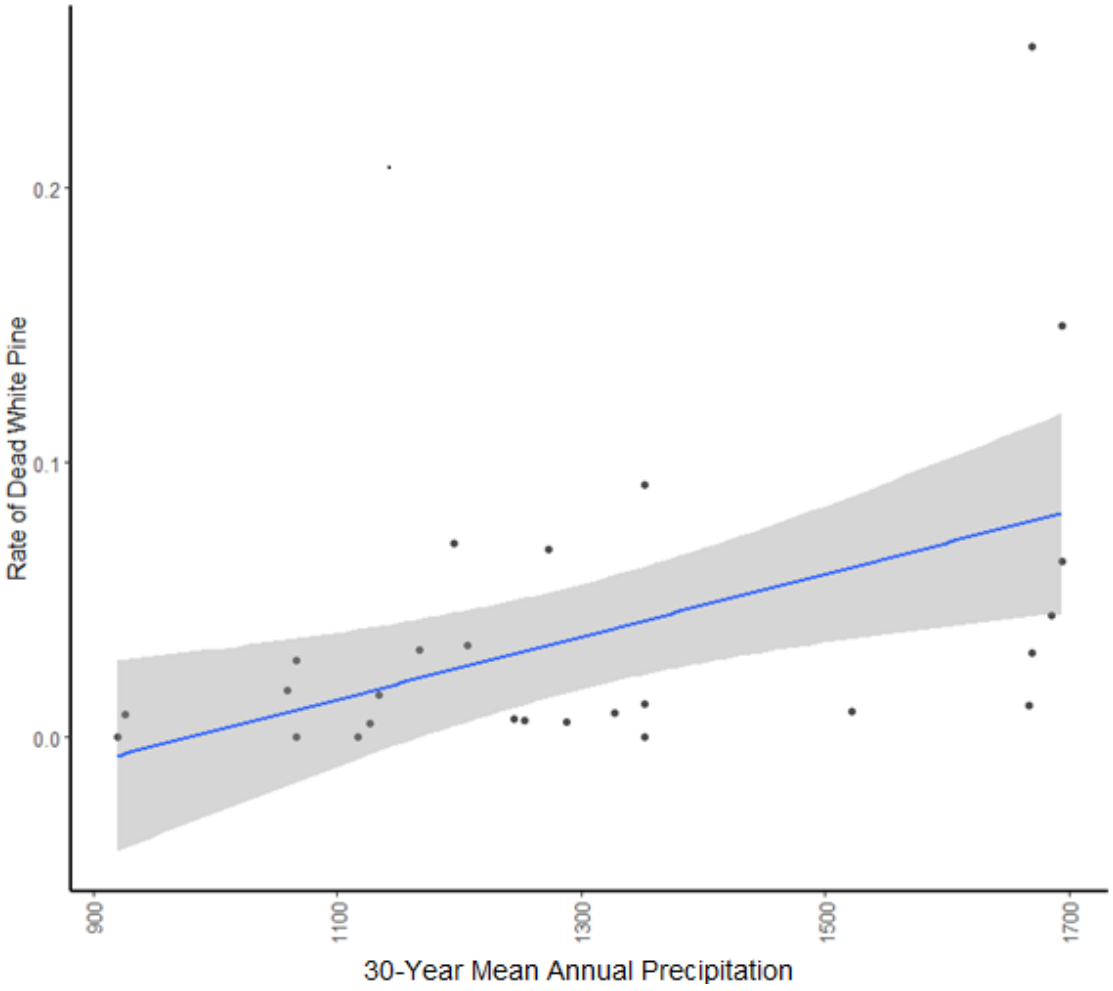

Appendix G 1. Rate of dead white pines (*Pinus lambertiana* and *Pinus monticola*) per plot by 30-year (1990-2020) mean annual precipitation, with blue trend line and shaded 95% confidence interval.